system would theoretically prevent false positives. Another of its advantages is that it can be applied directly to blood samples or extracted DNA. The purification of granulocytes from whole blood or bone marrow samples is not necessary. Therefore, the time needed to prepare and run these assays is also very short (<90 min) and simple, reducing technical biases among operators. In order to maximize the sensitivity, the sacrifice of precise quantitivity has been unavoidable. However, some quantitivity could potentially be gained via modifications to the existing QP-system.

Using the QP-system, the JAK2V617F mutation was detected in 25 specimens, but using direct sequencing, only 18 of those cases were detected (Table 1). The mutation was present in samples from PV and ET patients but was absent in all samples from secondary erythrocytemia and healthy volunteers. Each mutant specimen that was detected by direct sequencing was also detected by the QP-system. Importantly, there were 7 cases in which the mutation was identified by QP-system but not by direct sequencing (Fig. 3B(c), Table 1). These 7 cases were comprised of one PV (Case 2) and six ET (Case 10, 22, 23, 25, 30, 31) specimens. These specimens were further subjected to allele-specific PCR, which, while time-consuming and laborious, is the most sensitive existing detection method [6]. In each case, the allele-specific PCR results confirmed the QP-system findings (Table 1).

Recently, growing evidence has demonstrated the profound impact of particular genetic mutations on the pathogenesis, the diagnosis and treatment in various cancerous diseases. For example, mutations in the Abl kinase domain greatly impair the effect of the drug imatinib mesylate, an inhibitor of Abl tyrosine kinase, against chronic myeloid leukemia [8]. Thus, rapid and convenient detection of genetic mutations in individual patients will become more and more important for patient-oriented treatment. The present QP-system can be adapted theoretically to all mutations with only exchange of reagent cartridges (Fig. 1 and supplemental Fig. 1) which contain specific PCR primers and a QProbe designed for each mutation. Thus, the present QP-system may become a useful tool in the era of molecular targeting therapy.

In conclusion, with its high sensitivity, convenience and speed, the QP-system will enable point-of-care testing in clinical laboratories and patient-oriented therapy for not only for CMPDs but also for various cancers in the clinical field.

## Acknowledgments

This work was supported by Grants-in-Aid for Scientific Research from the Ministry of Education, Culture, Sports, Science, Technology of Japan, Japan Leukaemia Research Fund, Research Grant of the Princess Takamatsu Cancer Research Fund and Kobayashi Foundation for Innovative Cancer Chemotherapy. We are grateful to Dr. A. Roberts (The Walter and Eliza Hall Institute), Dr. O. Cooley (Royal North Shore Hospital), Dr. T. Akaogi and Dr. N. Sawai (Kyoto Second Red Cross Hospital) and Dr. T. Takahashi (Tokuyama Central Hospital) for scientific support.

*Contributions*: Ruriko Tanaka: research, analysis of data; Junya Kuroda: research, analysis data, composition of the paper; William Stevenson, Mitsuharu Hirai, Satoshi Majima, Takayuki Ishikawa, Tomohiko Taki, Yutaka Kobayashi, Eishi Ashihara, Yuri Kamitsuji, Eri Kawata, Miki Takeuchi, Yoshihide Murotani, Asumi Yokota, Masafumi Taniwaki: research; Taira Maekawa, Shinya Kimura: research design, composition of the paper.

## Appendix A. Supplementary data

Supplementary data associated with this article can be found, in the online version, at doi:10.1016/j.leukres.2007.12.019.

## References

[1] Tefferi A. Classification, diagnosis and management of myeloproliferative disorders in the JAK2V617F era. Hematol Am Soc Hematol Educ Program 2006:240–5.
[2] Li Z, Xu M, Xing S, et al. Erlotinib effectively inhibits JAK2V617F activity and polycythemia vera cell growth. J Biol Chem 2007;282:3428–32.
[3] Ito T, Tanaka H, Kimura A. Establishment and characterization of a novel imatinib-sensitive chronic myeloid leukemia cell line MYL, and an imatinib-resistant subline MYL-R showing overexpression of Lyn. Eur J Haematol 2007;78:417–31.
[4] Vardiman JW, Brunning RD, Harris NL. WHO histological classification of chronic myeloproliferative diseases. In: Jaffe ES, Harris NL, Stein H, Vardiman JW, editors. World health Organization classification of tumours: tumours of the haematopoietic and lymphoid tissues. Lyon, France: International Agency for Research on Cancer Press; 2001. p. 17–44.
[5] Matsumoto N, Kakihara F, Kimura S, et al. Single nucleotide polymorphism genotyping of CYP2C19 using a new automated system. Anal Biochem 2007;370:121–3.
[6] Stevenson WS, Hoyt R, Bell A, et al. Genetic heterogeneity of granulocytes for the JAK2 V617F mutation in essential thrombocythaemia: implications for mutation detection in peripheral blood. Pathology 2006;38:336–42.
[7] Poodt J, Fijnheer R, Walsh IB, Hermans MH. A sensitive and reliable semi-quantitative real-time PCR assay to detect JAK2 V617F in blood. Hematol Oncol 2006;24:227–33.
[8] Kimura S, Naito H, Segawa H, et al. NS-187, a potent and selective dual Bcr-Abl/Lyn tyrosine kinase inhibitor, is a novel agent for imatinib-resistant leukemia. Blood 2005;106:3948–54.

# Down-regulation of TCF8 is involved in the leukemogenesis of adult T-cell leukemia/lymphoma

*Tomonori Hidaka,[1,2] *Shingo Nakahata,[1] *Kinta Hatakeyama,[3] Makoto Hamasaki,[1,4] Kiyoshi Yamashita,[2] Takashi Kohno,[5] Yasuhito Arai,[6] Tomohiko Taki,[7] Kazuhiro Nishida,[7] Akihiko Okayama,[8] Yujiro Asada,[3] Ryoji Yamaguchi,[9] Hirohito Tsubouchi,[2,10] Jun Yokota,[5] Masafumi Taniwaki,[7] Yujiro Higashi,[11] and Kazuhiro Morishita[1]

[1]Division of Tumor and Cellular Biochemistry, Department of Medical Sciences, [2]Department of Internal Medicine II, University of Miyazaki, Miyazaki; [3]First Department of Pathology, Faculty of Medicine, University of Miyazaki, Miyazaki; [4]Miyazaki Prefectural Industrial Foundation, Miyazaki; [5]Biology Division, National Cancer Center Research Institute, Tokyo; [6]Cancer Genome Project, National Cancer Center Research Institute, Tokyo; [7]Department of Hematology and Oncology, Kyoto Prefectural University of Medicine, Kyoto; [8]Department of Rheumatology, Infectious Diseases and Laboratory Medicine, University of Miyazaki, Miyazaki; [9]Department of Veterinary Pathology, University of Miyazaki, Miyazaki; [10]Department of Digestive and Life-style related Disease, Kagoshima University Graduate School of Medicine and Dental Sciences, Kagoshima; and [11]Graduate School of Frontier Biosciences, Osaka University, Osaka, Japan

**Adult T-cell leukemia/lymphoma (ATLL) is caused by latent human T-lymphotropic virus-1 (HTLV-1) infection. To clarify the molecular mechanism underlying leukemogenesis after viral infection, we precisely mapped 605 chromosomal breakpoints in 61 ATLL cases by spectral karyotyping and identified frequent chromosomal breakpoints in 10p11, 14q11, and 14q32. Single nucleotide polymorphism (SNP) array–comparative genomic hybridization (CGH), genetic, and expression analyses of the genes mapped within a common breakpoint cluster region in 10p11.2 revealed that in ATLL cells, transcription factor 8 *(TCF8)* was frequently disrupted by several mechanisms, including mainly epigenetic dysregulation. *TCF8* mutant mice frequently developed invasive CD4+ T-cell lymphomas in the thymus or in ascitic fluid in vivo. Down-regulation of TCF8 expression in ATLL cells in vitro was associated with resistance to transforming growth factor β1 (TGF-β1), a well-known characteristic of ATLL cells, suggesting that escape from TGF-β1–mediated growth inhibition is important in the pathogenesis of ATLL. These findings indicate that *TCF8* has a tumor suppressor role in ATLL. (Blood. 2008;112:383-393)**

## Introduction

Adult T-cell leukemia/lymphoma (ATLL) is a peripheral CD4+ T-cell malignancy caused by infection with human T-lymphotropic virus-1 (HTLV-1).[1] HTLV-1 infection is endemic in a number of well-defined geographic regions within Japan, and as many as 20 million individuals worldwide are estimated to harbor it.[2] ATLL occurs after a prolonged latency period of up to 50 years in approximately 5% of individuals who have been infected with HTLV-1 around the time of birth. HTLV-1 encodes a transactivator, *Tax*, which plays a key role in the polyclonal growth of infected T cells through the activation of various genes.[3] However, recent studies have shown that Tax expression is undetectable in circulating ATLL cells, while a genetically and epigenetically defective provirus was observed in more than half of the ATLL patients examined.[4,5] Considering the long latency period of ATLL, it has been proposed that at least 5 additional genetic or epigenetic events are required for the development of overt disease.[1,6]

Nonrandom chromosomal translocations are considered to cause leukemic transformation, including structural and/or quantitative abnormalities of transcription factors such as *AML1, EVI1,* and *MLL*.[7] To identify disease-specific chromosomal translocations in ATLL, karyotypes of 107 ATLL cases determined by the G-banding method were reviewed in Japan.[8] There was a high degree of diversity and complexity, and disease-specific translocations were not found; however, translocations involving 14q32 (28%) or 14q11 (14%) and the deletion of 6q (23%) were the most frequent chromosomal abnormalities.[8] Recently, chromosome-based comparative genomic hybridization (CGH)[9] and BAC array-based CGH showed complex chromosomal abnormalities with gains in 1q, 2p, 4q, 7p, and 7q, and losses in 10p, 13q, 16q, and 18p.[10] To date, however, no gene involved in the development of ATLL has been isolated. Array CGH is useful for detecting genomic deletions or amplifications, but it cannot detect chromosomal translocations or inversions.

In this study, we searched for the existence of recurrent chromosomal rearrangements by multicolor spectral karyotyping (SKY) and high-resolution single nucleotide polymorphism (SNP) array-CGH (SNP array-CGH). We precisely mapped 605 chromosomal breakpoints in 61 ATLL cases. Breakpoints occurred most frequently in 10p11 and were mapped within a 1-Mb region in 10p11.2 with heterozygous deletions in all cases. A minimal common region of chromosome deletions, including a region of homozygous deletion, was mapped to a 2-Mb region. Genetic and expression analyses of the genes mapped within the deleted region revealed transcription factor 8 *(TCF8)* to be frequently altered in ATLL cells by several mechanisms, including mainly epigenetic dysregulation, suggesting that *TCF8* may be a candidate tumor suppressor gene. *TCF8* (GenBank accession number, NM 030751[11]), *AREB6, ZFHEP, NIL-2A, ZFHX1A, NIL-2-A, MGC133261,* or

Submitted January 5, 2008; accepted April 4, 2008. Prepublished online as *Blood* First Edition paper, May 8, 2008; DOI 10.1182/blood-2008-01-131185.

*T.H., S.N., and K.H. contributed equally to this paper.

The online version of this article contains a data supplement.

The publication costs of this article were defrayed in part by page charge payment. Therefore, and solely to indicate this fact, this article is hereby marked "advertisement" in accordance with 18 USC section 1734.

*ZEB1* encodes a 2-handed zinc finger homeodomain protein,[12] which represents a key player in pathogenesis associated with tumor progression in solid cancers.[13,14] In this study, we found that *TCF8* mutant mice frequently developed $CD4^+$ T-cell lymphoma/leukemia half a year after birth. Furthermore, we showed that down-regulation of TCF8 expression in ATLL cells in vitro was associated with TGF-β1 resistance, a well-known characteristic of ATLL cells, suggesting that escape from TGF-β1–mediated growth inhibition is one of the primary mechanisms in the pathogenesis of ATLL. These findings suggest that *TCF8* has an important tumor suppressor role in ATLL.

## Methods

### Patient samples

ATLL cells were collected from patients at the time of admission to hospital and before chemotherapy.[15] Diagnosis of ATLL was made on the basis of clinical features, hematologic characteristics, serum antibodies against HTLV-1 antigens, and insertion of the HTLV-1 viral genome into leukemia cells by Southern blot hybridization. Using Shimoyama's criteria,[16] all patients were diagnosed as acute-type ATLL. Mononuclear cells were obtained from heparinized blood or ascites by Histopaque density gradient centrifugation (Sigma-Aldrich, St Louis, MO). After separation, ATLL cell enrichment of more than 90% was confirmed by 2-color flow cytometric analysis. All samples were separated by Histopaque density gradient centrifugation, quickly frozen within 3 hours, and cryopreserved at −80°C. This study was approved by the Institutional Review Board of the Faculty of Medicine, University of Miyazaki. Informed consent was obtained from all blood and tissue donors in accordance with the Declaration of Helsinki.

### Cell lines

Acute lymphoblastic leukemia (ALL) cell lines used in this study were described previously.[15] Briefly, 4 of the cell lines, Jurkat, MOLT4, MKB1, and KAWAI, are HTLV-1–negative human T-cell acute lymphoblastic leukemia (T-ALL) cell lines.[17,18] Three cell lines, KOB, SO4, and KK1, are interleukin 2 (IL2)–dependent ATLL cell lines.[19] ED, Su9T, and S1T are IL2-independent ATLL cell lines.[20] MT2 and HUT102 are human T-cell lines transformed by HTLV-1 infection.[21] CTLL2 is a murine IL2–dependent T-lymphoma cell line.[22] All the cell lines were maintained in RPMI1640 medium supplemented with 10% fetal calf serum (FCS) and with or without IL2.

### Cell culture and karyotype analysis

G-banding studies were performed as described previously.[8] Briefly, leukemia cells were diluted in 10 mL RPMI1640 medium supplemented with 10% FCS at a final concentration of $10^6$ cells/mL. The cells were cultured at 37°C for 24 to 48 hours in humidified air with 5% $CO_2$, exposed to colcemid (0.05 mg/mL) for 60 minutes, processed in 0.075 M potassium chloride for 20 minutes, and fixed with methanol/glacial acetate (3:1). The chromosomes were treated with trypsin, stained with a Giemsa solution, and karyotyped according to the International System for Human Cytogenetic Nomenclature (ISCN 2005).[23] The remaining chromosome pellets were stored at −20°C for SKY and fluorescence in situ hybridization (FISH) analyses.

### SKY and DAPI banding analysis

The strategy of combined spectral karyotyping (SKY) and 4,6-diaminido-2-phenylindole dihydrochloride (DAPI) banding analysis of chromosome abnormalities was published[24] and is briefly described as follows: The chromosomes prepared on a slide glass were denatured and hybridized with a cocktail probe mixture for 2 days at 37°C. The SKY probe mixture and hybridization reagents were purchased from Applied Spectral Imaging (Vista, CA), and signal detection was performed according to the manufacturer's protocol. The chromosomes were counterstained with DAPI combined with an antifade solution (Vectashield; Vector Laboratories, Burlingame, CA). Images were acquired by an SD200 Spectracube (Applied Spectral Imaging) mounted on an Olympus BX50-RF (Olympus, Tokyo, Japan) using a custom-designed optical filter (SKY-1; Chroma Technology, San Diego, CA). With another special optical filter, the inverted DAPI images were captured in conjunction with spectral classifications as QFH band patterns for the identification of chromosomal breakpoints. For each case, 10 to 20 metaphase spreads were analyzed, and karyotypes were described according to the ISCN 2005.[23]

### FISH analysis

The plasmid library from sorted human chromosomes 10 (pBS10) was used as a whole chromosome painting (WCP) probe, labeled with digoxigenin-16-dUTP (Boehringer-Ingelheim, Ingelheim, Germany) by standard nick translation. BAC clones were labeled with biotin-16-dUTP (Sigma-Aldrich). Hybridization and signal detection were performed as described previously.[25] A minimum of 50 nuclei was examined for each FISH. FISH analysis was performed on metaphase and interphase chromosomes by 53 BAC clones mapped to the chromosome bands 10p11-12 in the human genome mapping of NCBI (build 36 version 1)[26] as probes.

### High-density SNP array comparative genomic hybridization (array-CGH) analysis

Total genomic DNA was digested with *Xba*I, ligated to an adaptor, and subjected to polymerase chain reaction (PCR) amplification using a single primer. After treatment with DNase I, 40 μg of the PCR products was labeled with a biotinylated nucleotide analog and hybridized the microarray. SNP genotypes were scored with the GTYPE 4.1 software (Affymetrix, Santa Clara, CA). Chromosome copy number and LOH were calculated with 2 programs, ACUE 2.1 (Mitsui Knowledge Industry, Tokyo, Japan, http://bio.mki.co.jp/en/product/acue2/index.html) and CNAG 2.0 (Affymetrix).[27] For data normalization, we used 6 normal reference samples. Genomic location of probes on the array was determined with the information in NCBI genome map build 35.1.[26]

### Mice

C57BL/6 and ICR mice were purchased from CLEA Japan (Tokyo, Japan) and maintained under specific pathogen-free conditions. The targeted allele of the δ*EF1* gene, the murine orthologue of *TCF8*, lacks only the COOH-proximal zinc finger cluster domain.[28] Approximately 20% of the homozygous *TCF8* mutant mice were born alive and grew up to adulthood, although it was reported to cause a defect in the thymic T-cell development.[28,29] To produce viable homozygous *TCF8* mutant mice, we made their genetic backgrounds more heterogeneous by crossing the C57BL/6 background *TCF8* mutant mice with the ICR outbred strain or F1 (C57BL/6 × C3H) mice.

### Assay for cell proliferation

Control siRNA was purchased from Qiagen (Valencia, CA; AllStars Negative Control [ANC] siRNA) and the *TCF8* siRNA was from Ambion (Austin, TX; murine *TCF8;* 5′-CCUGUGGAUUAUGAGUUCA-3′, human *TCF8* 5′-GGGUUACUUGUACACAGCU-3′). For the construction of vectors expressing TCF8, human *TCF8* cDNA was subcloned into pCMV26 (Sigma-Aldrich). The cells were transiently transfected using the Nucleofector Kit (Amaxa, Gaithersburg, MD) according to the manufacturer's recommendations. The transfection efficiency, evaluated by fluorescence microscopy of green fluorescent protein, was more than 80%. Twenty-four hours after transfection, the expression of TCF8 protein in the cells was investigated by Western blotting, while for the cell proliferation studies, each transfectant was plated at a density of $4 \times 10^3$ cells per well in 96-well microtiter plates. The cells were treated with various concentrations of transforming growth factor (TGF-β1; R&D Systems, Minneapolis, MN) for 72 hours and counted by the methyl thiazolyl tetrazolium (MTT) assay

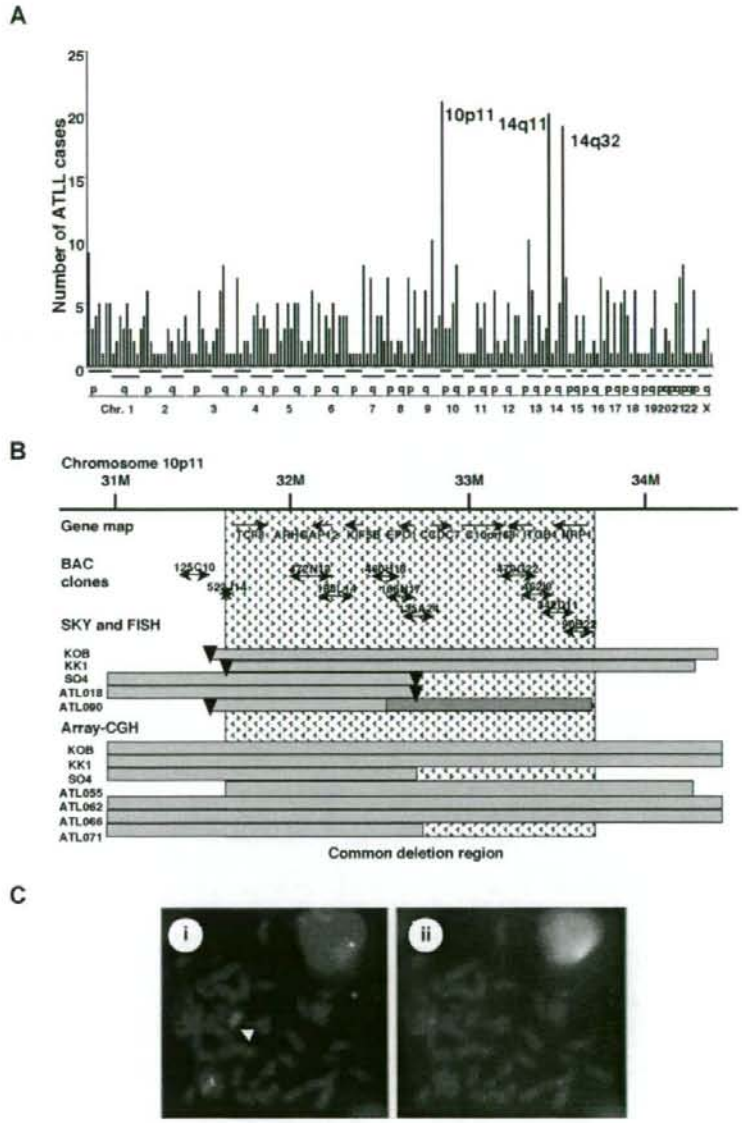


**Figure 1. Mapping of the deletions at 10p11.2.** (A) Mapping of the chromosomal breakpoints in whole chromosomes in acute-type ATLLs. An analysis of the chromosomal breakpoints was performed by spectral karyotyping (SKY), and all chromosomal breakpoints were mapped in each region of the chromosomes (x-axis), as indicated at the bottom. The y-axis shows the numbers of ATLL cases with the chromosomal breakpoints in each chromosomal region. Three regions, 10p11, 14q11, and 14q32, were frequently identified with chromosomal breakpoints. (B) Physical and transcriptional maps of the region containing the chromosomal deletion at 10p11. A FISH analysis was performed on metaphase and interphase chromosomes using 53 BAC clones mapped to the chromosome bands at 10p11-12 in the human genome map of NCBI (build 36 version 1[26]) as probes. The bars indicate the region covering each BAC clone. Horizontal bars indicate the region with hemizygous deletions in each DNA sample from the ATLL cell lines or ATLL cells from patients, which were detected by SKY and FISH or array-CGH analyses. The inverted triangles indicate the regions of chromosomal breakpoints. Closed bars indicate the region of a homozygous deletion in a DNA sample from ATLL cells (ATL090). The hatch pattern represents the minimal heterozygous deletion at 10p11.2. *TCF8* through *NRP1* represent the names of the genes within the region in the human genome map of NCBI (build 36 version 1[26]). (C) FISH validation of the RP11-188L14 probe to detect the hemizygous deletion of the chromosome10p11.2 in SO4 cell line. The RP11-188L14 probe was green (FITC) and the whole chromosome painting probe was red (TRITC). FISH with RP11-188L14 shows no signal on the abnormal chromosome 10 as indicated by the arrow (i), and a DAPI photograph corresponding to the FISH picture is shown on the right side (ii). Images were captured through the oil objective lens (100×) with a CCD camera (SenSys 0400-GI; Photometrics Ltd, Tucson, AZ). Subsequent image processing was performed with the Software IPLab version 2.4.0 (BD Biosciences Bioimaging, Rockville, MD).

using Tetra color one assay kit (Seikagaku Kogyo, Tokyo, Japan). Each experiment was performed 3 times, and typical results are shown.

## Results

### Identification of a common hemizygous deletion in 10p11 in ATLL by mapping chromosomal breakpoints

We recently studied recurrent chromosomal rearrangements in adult T-cell leukemia lymphoma (ATLL) cells from 61 patients by spectral karyotyping (T.H. et al, manuscript in preparation). In examining the molecular changes in ATLL cells, 605 chromosomal breakpoints in 61 cases were identified and precisely mapped by DAPI banding analysis. The frequency of the breakpoints was counted in each region of the chromosomes, with an average of around 10 translocations in each case (Figure 1A). Most of the chromosomal translocations were unbalanced, and a few recurrent reciprocal translocations were found. Chromosomal breakages were most frequently identified at 10p11 (21 [34.6%] of 61 cases), and they were also frequently represented at 14q11 and 14q32 regions (Figure 1A). Based on the data of SKY, these 3 events occurred almost independently; however, almost 50% of the cases with 14q32 abnormality demonstrated a 10p11.2 abnormality, suggesting that both events are interrelated chromosomal abnormalities. The 10p11 regions were translocated to more than 10 different partner chromosomal regions, such as 21q22, 13q14, and 14q32.

Therefore, we precisely mapped the chromosomal breakpoints at 10p11 in 3 ATLL cell lines (KK1, KOB, and SO4) and 2 primary ATLL cases (ATL018 and ATL090) by FISH. We identified der(10)t(10,22)(p11.2;q13.1) in KK1, der(10)t(10,14)(p11.2;q11.2)

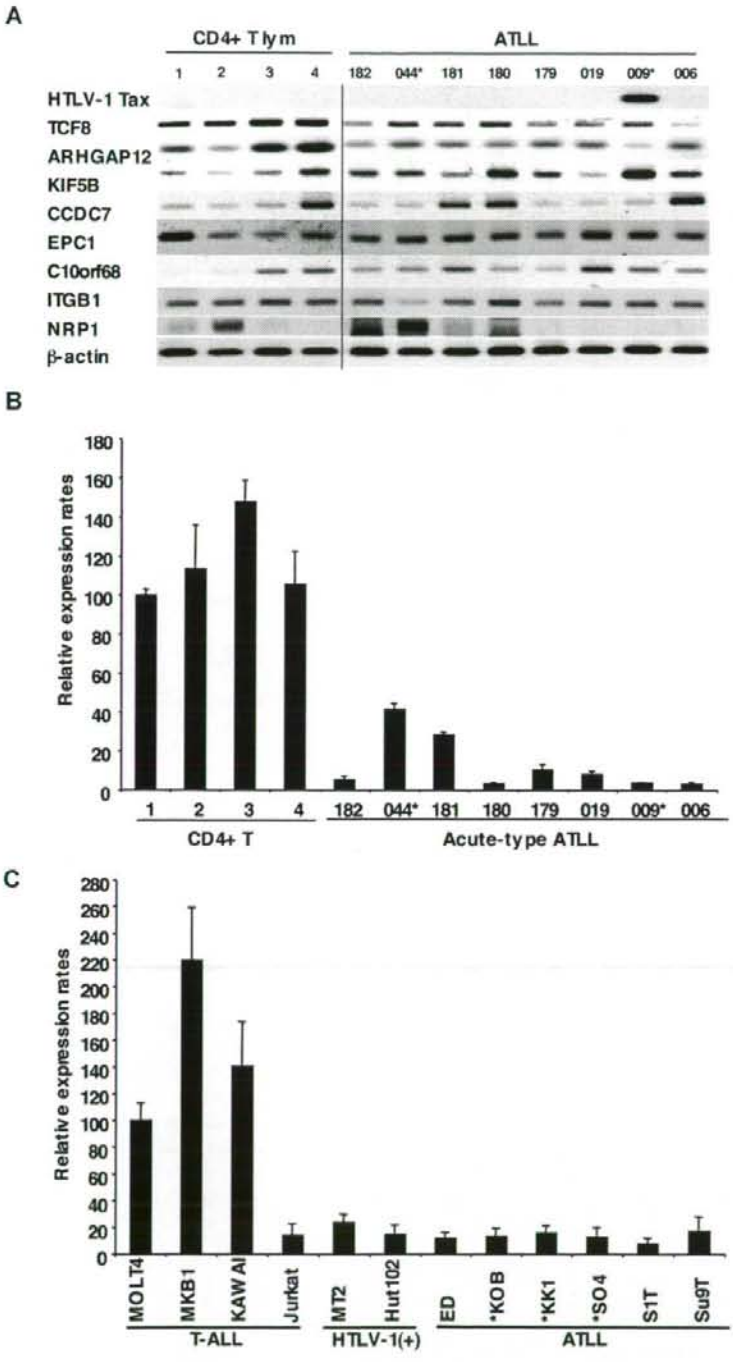


**Figure 2. Down-regulated expression of *TCF8* in ATLL cells.** (A) The expression profiles of the genes mapped within the deletion region at 10p11. Semiquantitative reverse-transcription PCR (RT-PCR) was performed to determine the expression of the genes mapped within the deletion region. *TCF8, ARHGAP12, KIF5B, CCDC7, EPC1, C10orf68, ITGB1,* and *NRP1* showed a single band of amplified cDNA from CD4+ T lymphocytes from healthy volunteers as controls and from ATLL cells from the patients. A band of HTLV1 *Tax* was amplified from only 1 of 8 ATLL cells. A vertical line has been inserted to indicate a repositioned gel lane. (B) Quantitative RT-PCR analysis of *TCF8* mRNA in 4 samples of CD4+ T lymphocytes from healthy volunteers and 8 samples of ATLL cells from the patients. The data were normalized to *β-actin* mRNA and calibrated to the *TCF8*/*β-actin* ratio (ΔCT) in the case of healthy volunteer no. 1, as a relative expression rate of 100. The data are the mean and standard deviation of $2^{-\Delta\Delta CT}$ in a duplicate assay. Two patients (indicated by *) have the chromosome 10p11.2 abnormalities. (C) Quantitative RT-PCR analysis of *TCF8* mRNA in various types of T lymphoblastic leukemia cell lines. MOLT4, MKB1, KAWAI, and Jurkat are T-lymphoid leukemia cell lines; MT2 and HUT102 are HTLV-1–infected cell lines; and ED, KOB, KK1, SO4, S1T, and Su9T are ATLL cell lines. Three ATLL cell lines (indicated by *) showed the deletion of chromosome 10p11.2 with *TCF8*.

in KOB, der(10)t(2;10)(p23;p11.2) in SO4, t(10;21)(p11.2;q11.2) in ATL018, and t(10;13)(p11.2;q14) in ATL090 (Table S1, available on the *Blood* website; see the Supplemental Materials link at the top of the online article). Using 53 BAC clones on 10p as DNA probes for FISH (Table S2), the chromosomal breakpoints in these 5 cases were mapped to a 1-Mb region at 10p11.2 (Figure 1B). It was noted that the genomic deletions surrounding the chromosomal breakpoints were detected by a FISH analysis (Figure 1C) and heterozygous deletions of the 10p11.2 region with translocations were found in all 5 samples (Table S2; Figure 1B). Heterozygous deletions of approximately 2 to 8 Mb in the 10p11.2 region with translocations were found in all 5 samples. In addition, no FISH

**Table 1. Summary of the genetic and epigenetic abnormalities in ATLL cell lines**

| Cell line | Cell type | 10p abnormalities | Point mutation | Treatment | | |
|---|---|---|---|---|---|---|
| | | | | 5-Aza-dC, fold ± SD | TSA, fold ± SD | 5-Aza-dC+TSA, fold ± SD |
| MOLT4 | T-ALL | None | None | 1.25 ± 0.46 | 1.65 ± 0.21 | 1.65 ± 0.22 |
| Jurkat | T-ALL | None | None | 11.17 ± 0.59* | 10.04 ± 1.74* | 3.07 ± 0.54* |
| MT2 | HTLV-1 (+) | None | None | 3.38 ± 1.17* | 8.25 ± 1.76* | 4.58 ± 0.90* |
| HUT102 | HTLV-1 (+) | None | 255A>C Asn78Thr | 4.39 ± 0.49* | 6.94 ± 0.16* | 8.03 ± 1.05* |
| ED | ATLL | None | None | 4.32 ± 1.57* | 7.48 ± 0.91* | 3.93 ± 0.21* |
| KOB | ATLL | 10p del | None | 3.26 ± 1.12* | 2.32 ± 0.81 | 2.08 ± 0.54 |
| KK1 | ATLL | 10p del | None | 9.92 ± 0.45* | 6.76 ± 0.17* | 9.72 ± 0.35* |
| SO4 | ATLL | 10p del | None | 1.40 ± 0.33 | 1.57 ± 0.18 | 0.59 ± 0.06 |
| S1T | ATLL | None | None | 3.66 ± 0.21* | 3.95 ± 0.75* | 2.32 ± 1.63 |
| Su9T | ATLL | None | None | 3.91 ± 0.45* | 9.66 ± 2.38* | 1.42 ± 0.21 |

Data are means plus or minus SD.
*$P < .05$ versus control (Dunnett test).

signals were detected in the 1-Mb region from RP11-135A24 to RP11-462L8 in ATL090, suggesting that a 10p11 region-specific homozygous deletion had occurred in this case (Figure 1B). Therefore, a minimal common region of chromosome deletions, including a region of homozygous deletion in ATL090, was mapped to a 2-Mb region from PR11-523J14 to RP11-342D11 (Figure 1B).

To confirm these results, we performed SNP array-CGH using DNA from 8 ATLL-related cell lines including KK1, KOB, SO4, and an additional 10 samples from acute-type ATLL patients. Deletions in 10p11.2, including the 2-Mb deletion region, were noted in 3 cell lines: KK1, KOB, and SO4, and an additional 4 patient samples (Figure 1B; Table S3). Using SNP array-CGH, the telomeric deleted regions in chromosome 10p11.2 in KOB and KK1 covered a wider area than those detected by FISH analysis, and each deleted region in the 3 cell lines and 4 patients samples covered the common deletion region. To combine these data, the same minimal common region of chromosome deletions, including regions of homozygous deletion in ATL090, was mapped to a 2-Mb region from PR11-523J14 to RP11-342D11 (Figure 1B), suggesting that a tumor suppressor gene possibly exists in this 2-Mb region in 10p11.2.

### Down-regulation of *TCF8* mRNA in ATLL cells

We examined the mRNA expression profiles of all 12 genes within the commonly deleted region in 10p11.2, which were identified by NCBI and Celera gene maps (Rockville, MD). Since mRNA samples from the ATLL patients used for the deletion mapping were not available, we initially used the mRNA expression profiles of the other 8 leukemia cell samples from acute-type ATLL patients by semiquantitative reverse-transcription PCR (RT-PCR), which had been previously identified by DNA microarray.[15] Two leukemia samples from patients with ATLL had chromosome 10p11.2 abnormalities: t(10;15) (p11.2;q26) in ATL044 and monosomy 10 in ATL009 (Table S1). Expression levels of 8 genes (*TCF8, ARHGAP12, KIF5B, CCDC7, EPC1, C10orf68, ITGB1* and *NRP1*) and HTLV-1 *Tax* as well as *β-actin* are shown in Figure 2A. The results showed that levels of *TCF8* mRNA in ATLL cells had a tendency to be lower than those in $CD4^+$ T lymphocytes from healthy volunteers, even though only 2 of 8 patients had chromosome 10p11.2 abnormalities. Other genes did not show any differences in expression level between the 2 groups. Expression profiles of the leukemia cells using a DNA microarray gave the same results (Figure S1), and quantitative real-time RT-PCR also showed that the expression level of *TCF8* mRNA in ATLL cells was significantly lower than that in $CD4^+$ T lymphocytes (Figure 2B).

To confirm these results, 12 T-ALL cell lines containing 6 ATLL cell lines (ED, KOB, KK1, SO4, S1T, and Su9T), 2 HTLV-1–infected T-cell lines (MT2 and HUT102), and 4 HTLV-1–uninfected T-ALL cell lines (Jurkat, MOLT4, MKB1, and KAWAI) were used for an expression study. Three cell lines (KOB, KK1, and SO4) revealed the deletion of chromosome 10p11.2 with *TCF8*. Although no other genes except *TCF8* showed any change in expression level in these cell lines (Figure S2), the expression level of *TCF8* was specifically down-regulated in all of the ATLL cell lines along with Jurkat cells by quantitative real-time RT-PCR (Figure 2C). These data suggest that *TCF8* transcription might be down-regulated by epigenetic inactivation in most ATLL-related cell lines with Jurkat cells.

### Increased expression of *TCF8* by 5-aza-2′-deoxycytidine or trichostatin A in ATLL cell lines

To clarify whether DNA methylation and/or histone deacetylation of the *TCF8* gene promoter were involved in the transcriptional repression of *TCF8* in ATLL cell lines with Jurkat cells, 10 cell lines (2 T-ALL, 2 HTLV-1–infected, and 6 ATLL-derived cell lines) were cultured with (1) 10 μM 5-aza-2′-deoxycytidine (5-aza-dC), a DNA demethylating agent, for 72 hours, (2) 1.2 μM trichostatin A (TSA), an inhibitor of histone deacetylase, for 48 hours, or (3) 1.2 μM TSA for 48 hours following culture with 10 μM 5-aza-dC for 24 hours. After treatment with 5-aza-dC, *TCF8* expression was up-regulated in 8 of 10 cell lines (Jurkat, MT2, HUT102, ED, KOB, KK1, S1T, and Su9T), with more than 3-fold activation ($P < .05$) as detected by real-time RT-PCR (Table 1). After treatment with TSA for 48 hours, the levels of *TCF8* mRNA increased in 7 of 10 cell lines (Jurkat, MT2, HUT102, ED, KK1, S1T, and Su9T), also with more than 3-fold activation ($P < .05$). In addition, combination therapy induced *TCF8* mRNA expression in 5 cell lines by more than 3-fold. Therefore, *TCF8* mRNA expression was activated in 7 of 8 ATLL-related cell lines along with Jurkat cells by either 5-aza-dC or TSA treatment, suggesting that the down-regulation of *TCF8* in most of the ATLL cell lines except SO4 cells with a chromosome 10p hemizygous deletion was dependent on epigenetic abnormalities.

### Unmethylated putative *TCF8* promoter in ATLL cell lines

Next, we determined the methylation status of the *TCF8* promoter by bisulfite sequencing. A CpG island containing 50 CpGs was

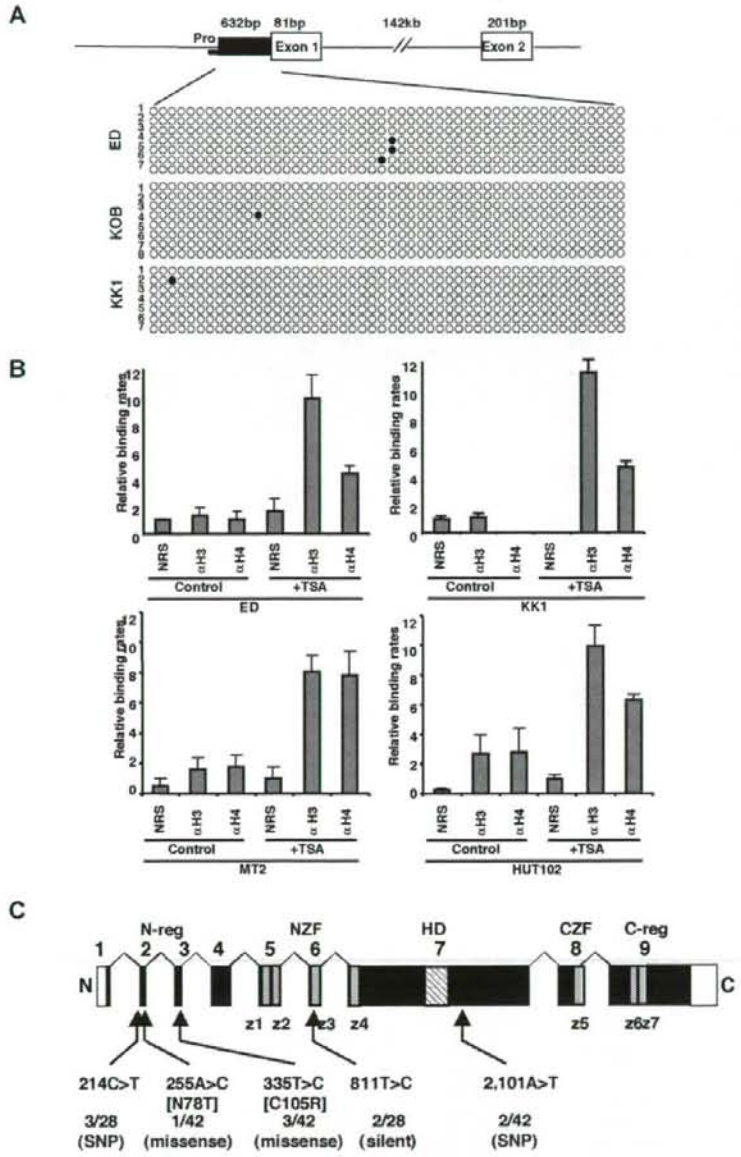


**Figure 3. Genetic and epigenetic abnormalities of the *TCF8* gene in ATLL cells.** (A) Bisulfite genomic sequencing of the *TCF8* promoter region in 3 ATLL cell lines: ED, KOB, and KK1. PCR products amplified from bisulfite-treated DNA were subcloned, and 8 clones in each cell line were sequenced. ○ indicate unmethylated CpGs (Thy), and ● indicate methylated CpGs (Cyt). The sequenced region contains 50 CpGs in 632 bp, just upstream from exon 1. Pro indicates a region of the *TCF8* promoter for chromatin immunoprecipitation. (B) Specific DNA binding of acetylated histone H3 or H4 to the *TCF8* promoter region detected by chromatin immunoprecipitation (ChIP). Two genomic DNA fragments containing every possible DNA-binding site, *TCF8* promoter, or *β-actin* promoter were amplified from the genomic DNA of fixed ATLL-related cell lines (MT2, HUT102, ED, and KK1) after immunoprecipitation with normal rabbit serum (NRS) or with antiacetylated histone H3 or H4 antibodies (αH3 or αH4). Quantitative PCR data calibrated to the *TCF8* promoter/*β-actin* ratio are shown in the NRS as a relative expression rate of 1. Data are the means plus or minus standard deviation of $2^{-\Delta\Delta Ct}$ in a duplicate assay. Cell lines were cultured in RPMI1640 medium containing 10% FCS with (+ TSA) or without (control) 1.2 μM TSA. (C) Genomic structure of the *TCF8* gene with a missense mutation and single nucleotide polymorphisms. Locations of the mutations and the single nucleotide polymorphisms relative to the exons encoding the functional domains are shown. *TCF8* encodes a homeodomain (HD) flanked by 2 zinc-finger clusters (z1 to z4 and z5 to z7) (NZF indicates N-terminal zinc finger repeats, CZF; C-terminal zinc finger repeats). The N-terminal transcriptional regulatory domain (N-reg) could bind to p300/CBP and the C-terminal transcriptional regulator domain (C-reg) is the region where acidic amino acids are clustered just after the last zinc-finger domain. Values represent the number of mutated cases per total number of tested cases. SNP indicates single nucleotide polymorphism. White boxes represent noncoding regions in exons 1 and 9.

amplified from a 632-bp region of the putative *TCF8* promoter adjacent to exon 1 using 2 pairs of PCR primers and bisulfite-treated genomic DNA from 3 ATLL cell lines: ED, KOB, and KK1. However, the *TCF8* promoter was not methylated in any of the 3 ATLL cell lines in which *TCF8* expression was induced by 5-aza-dC (Figure 3A), suggesting that the CpG island was not a direct target for DNA methylation in ATLL cells. Moreover, *TCF8* mRNA was up-regulated in various ATLL cell lines after treatment with hydralazine, which was reported to decrease DNA methyltransferase expression (Figure S3). This observation suggests that a transactivating regulator of *TCF8* may be modulated by methylation or the other regulatory elements are located outside the *TCF8* promoter. Such enhancer-related methylation events have been described for the imprinting of *H19* and *Igf2*, *p21WAF1* regulation by *p73*, and *Apaf-1*.[30-33] Therefore, further analyses will be needed to determine the exact regulatory element near the *TCF8* gene or to find a transactivating regulator of *TCF8*, which is directly methylated in ATLL cells.

### Histone deacetylation is directly involved in down-regulation of *TCF8* mRNA expression in ATLL cells

To confirm the correlation between reduced *TCF8* mRNA expression and histone deacetylation, *TCF8* expression and histone acetylation status were analyzed in the ATLL-related cell lines (MT2, HUT102, ED, and KK1) by chromatin immunoprecipitation (ChIP) after treatment with or without TSA. After treatment with TSA for 48 hours, the chromosomal DNA precipitated by antiacetylated histone H3 or H4

antibody was amplified with 2 sets of primers for the *TCF8* promoter region or for the human *β-actin* promoter region (Figure 3B). Band intensities of the *TCF8* promoter region in 4 cell lines were amplified 3- to 6-fold after treatment with TSA, indicating that histone deacetylation of the *TCF8* promoter region was directly involved in the down-regulation of *TCF8* mRNA expression in ATLL cells.

### Identification of missense mutations in *TCF8* in ATLL cells

We then searched for somatic *TCF8* mutations in DNA samples from 34 patients with acute-type ATLL and 10 T-cell leukemia cell lines. Genomic PCR did not detect any homozygous deletions in any of the 9 coding exons of *TCF8* in these samples. We detected 5 types of nucleotide substitutions, and all were heterozygous (Figure 3C). The 255A>C substitution in HUT102, creating a missense mutation (Asn78Thr) in exon 2, and the 335T>C substitution in the leukemia cells from 3 ATLL patients, creating a missense mutation (Cys105Arg) in exon 3, were likely to be somatic mutations (Table S4), since they were not detected in noncancerous cells from 95 Japanese volunteers.

The results of genomic and expression analysis indicate that the *TCF8* gene is altered by several mechanisms, including hemizygous deletion, epigenetic dysregulation, and intragenic mutations. Regarding the ATLL-related cell lines, 3 of 9 showed hemizygous deletions of 10p11.2; 8 of 9 showed epigenetic dysregulation of the *TCF8* gene; and 1 of 9 showed an intragenic mutation (Table 1). Therefore, *TCF8* is a strong candidate tumor suppressor gene for ATLL leukemogenesis and is initially inactivated by unbalanced translocations with heterozygous deletion in the 10p11.2 region in ATLL cells.

### Development of CD4+ T-cell lymphoma in *TCF8* mutant mice

To determine whether down-regulation of the *TCF8* gene could be a causative event for leukemogenic conversion of T lymphocytes to leukemia-lymphoma cells, we investigated δ*EF1* (mouse homologue of *TCF8*) gene-targeted mutant mice, which lack the COOH-proximal zinc finger clusters ($\delta EF1^{\Delta C\text{-}fin}$ allele) and were reported to have a defect in the thymic T-cell development.[28,29] Since 20% of the homozygous *TCF8* mutant mice were born alive, we made their genetic backgrounds more heterogeneous by crossing the C57BL/6 background with the ICR or F1 (C57BL/6 × C3H) mice. Homozygous mice on a mixed genetic background were born with almost normal Mendelian frequencies (wild-type: heterozygote:homozygote = 60:91:42). After 4 months, almost half of the *TCF8* homozygous mutant mice experienced enlargement of the abdomen due to ascites (27 [64.3%] of 42 mice), and many mice developed lymphomas with a median onset of disease of 30 weeks after birth and an earliest onset at 95 days after birth (Figure 4A). Half of the mice died within a year, and 84% of them developed fatal T-cell lymphomas. In *TCF8* homozygous mutant mice, 2 types of lymphomas were observed: (1) peripheral lymphomas with or without ascites, and (2) thymic tumors. Typical pathological findings of 15 mice (no. 6 to no. 21) are shown in Table S5. In the peripheral lymphoma group, a large amount of bloody or milky ascitic fluid had collected in approximately 60% of the mice with invasion of various organs (Figure 4B,C). Numerous lymphoma cells with medium to large, cleaved or noncleaved nuclei were observed in the ascitic fluid (Figure 4D). Lymphoma cells had invaded various lymph nodes, including the thoracic, peripancreatic, mesenteric, perirenal, mesenteric, and other peripheral lymph nodes (Figure 4E). Fluorescence-activated cell sorter

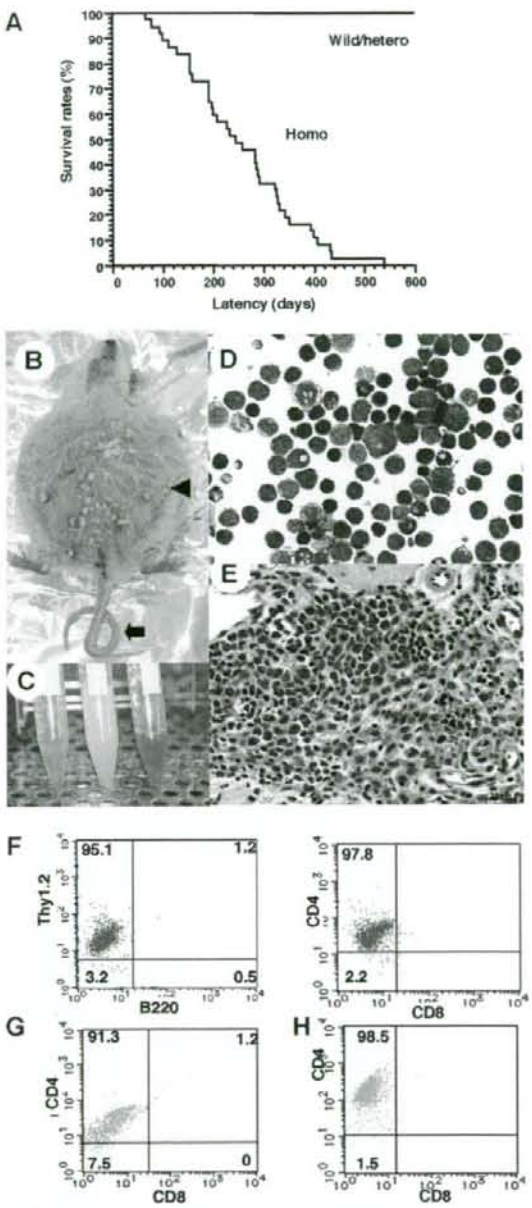


**Figure 4. Survival rates and pathologic findings in *TCF8* mutant mice.** (A) The survival rates of a cohort of wild-type (wild), *TCF8* heterozygous (hetero), and *TCF8* homozygous (homo) mutant mice were followed over the indicated period using Kaplan-Meier plots. (B) Gross photograph of *TCF8* mutant mice with ascites (◀). Approximately 30% of *TCF8*-homologous mutant mice showed curled tail (◆). (C) Bloody or milky ascites was pooled. (D) May-Giemsa staining of tumor cells in ascites. Original magnification ×400. (E) Many lymphoma cells with medium- to large-sized nuclei infiltrated in the mesentery. Cells were examined using an Axioskop 2 plus inverted microscope (Carl Zeiss, Rugby, United Kingdom) and digital images were aquired using AxioCam camera and AxioVision 2.05 software (Carl Zeiss). Original magnification ×400. (F) Tumor cells from ascitic fluids were analyzed by staining with a combination of monoclonal antibodies, either Thy1.2-PE with B220-FITC (left) or CD4-PE with CD8-FITC (right) and FACS. (G,H) The tumor cells that invaded liver (G) or spleen (H) were analyzed by staining with a combination of monoclonal antibodies, CD4-PE with CD8-FITC.

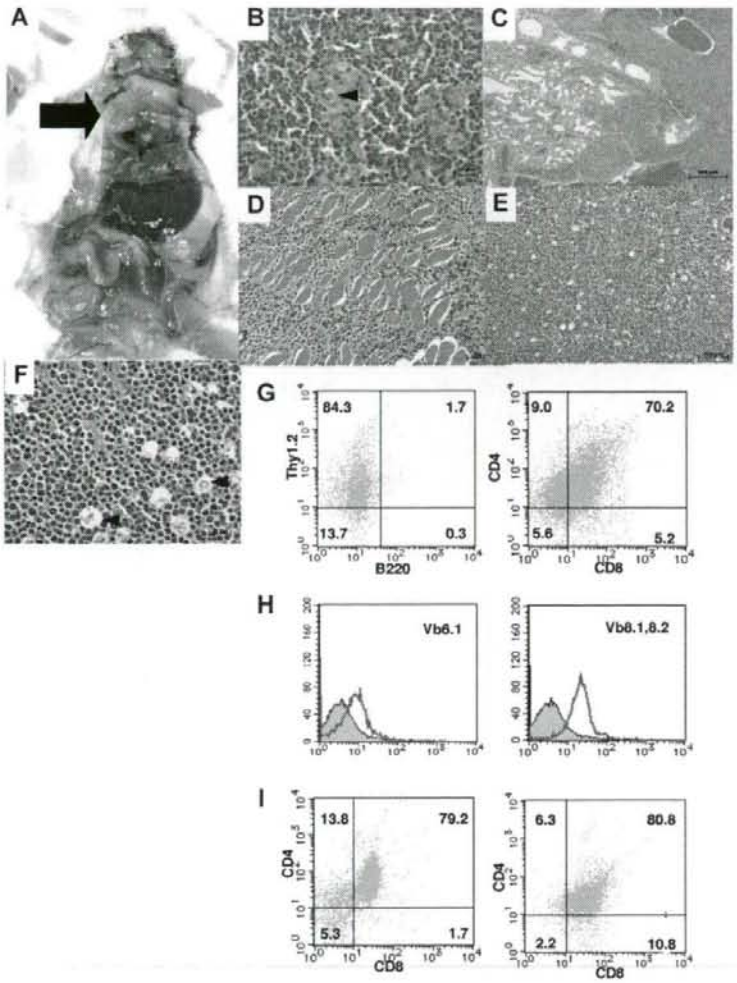


**Figure 5. Pathological findings of *TCF8* mutant mice.** (A) Gross autopsy of *TCF8* mutant mice with thymic tumors. A large thymic tumor (➔) was observed at the mediastinum of the dissected mouse. (B) Hematoxylin and eosin staining of tumor sections from the mouse as indicated. The normal thymic cellular architecture in the *TCF8* mutant mice is replaced with monotonous fields of large, highly mitotic lymphoblasts with small Hassall bodies (◀). The scale bar indicates 20 μm. Original magnification ×400. (C) The tumor cells invaded the lung, vascular tissues, and heart in the mouse. The scale bar indicates 500 μm. Original magnification ×25. (D) The tumor cells invaded the muscular tissues of the chest wall. The scale bar indicates 50 μm. Original magnification ×200. (E) Hematoxylin and eosin staining of peripheral lymph nodes. Tumor cells showed a diffuse proliferation of monomorphic lymphoma cells, focally mixed with tingible body macrophages ("starry-sky appearance") (◀). The scale bar indicates 100 μm. Original magnification ×100. (F) Hematoxylin and eosin staining of peripheral lymph nodes. The scale bar indicates 20 μm. Original magnification ×400. (G) Tumor cells from the thymic tumor were analyzed by staining with a combination of monoclonal antibodies, either Thy1.2-PE with B220-FITC (left) or CD4-PE with CD8-FITC (right) and FACS. (H) The tumor cells of the $CD3^+B220^-$ population did not express Vβ6.1 TCR (left), but showed weak expression of Vβ8.1-8.2 TCR (right). (I) Tumor cells from the liver (left) or spleen (right) were analyzed by staining with a combination of monoclonal antibodies, CD4-PE and CD8-FITC.

(FACS) analysis of the tumor cells showed that most of the lymphoma cells in the ascitic fluid and those that had invaded various organs were $CD4^+$ SP T cells (Figure 4F-H).

In the thymic tumor group, 16% of the homozygous mutant mice had large thymic tumors with a diameter of 1 to 3 cm (Figure 5A). Histologic analysis of the thymic tumors revealed that lymphoblastic lymphoma cells had densely proliferated in the cortex and medulla of the thymus (Figure 5B). Thymic lymphoma cells continuously invaded the lungs, chest wall, and pericardium (Figure 5C,D). In the peripheral lymph nodes, there was diffuse proliferation of monomorphic lymphoma cells focally mixed with tingible body macrophages, giving a "starry-sky" appearance (Figure 5E,F). In the thymic tumor group, surface marker analysis of thymic lymphoma cells revealed $CD4^+CD8^+$ DP T lymphoma cells (Figure 5G), which were negative for Vβ6.1 TCR and weakly positive for Vβ8.1-8.2 TCR with a single peak (Figure 5H). In this mouse, the mononuclear cells that invaded the liver, as well as a majority of the cells that invaded the spleen, were DP T lymphoma cells (Figure 5I). Therefore, in the same mouse, both tumor cells derived from the thymus and those that had invaded the organs were revealed to be DP T lymphoma cells. Moreover, the remaining mice with large thymic tumors showed the same $CD4^+CD8^+$ DP T lymphoma cells. In total, 84% of the T-cell tumors in *TCF8* homologous mutant mice could be classified as $CD4^+$ SP T-cell lymphoma, and 16%, as $CD4^+CD8^+$ DP thymic T-cell lymphoma. $CD8^+$ SP T lymphomas were never observed. Thus, the histopathological and cellular findings revealed that $CD4^+$ T-cell lymphoma/leukemia developed in most *TCF8* mutant mice.

### Down-regulation of TCF8 expression is associated with TGF-β1 resistance in ATLL cells

The TGF-β superfamily is known to inhibit the lineage commitment of double-positive (DP) cells toward $CD4^+$ T-cell differentiation.[34] Interestingly, the ATLL cells were found to be resistant to growth inhibition by TGF-β1, even with high levels of TGF-β1 expression,[35-37] suggesting that ATLL cells may have developed several mechanisms of resistance to escape the antiproliferative and inactivating signal mediated by TGF-β1, including Tax through activation of the JNK/c-Jun pathway[38,39] or MEL1S expression.[37] Since TCF8 is reported to synergize with Smad

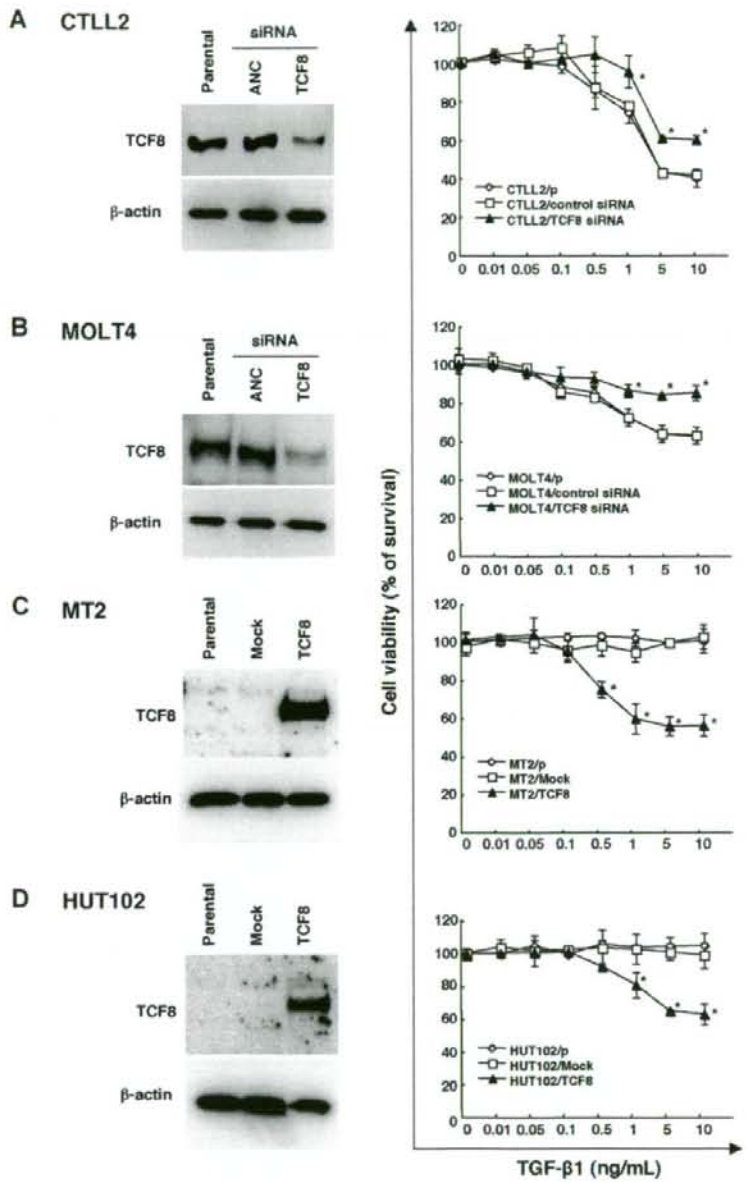


**Figure 6. TGF-β1 responsiveness in various leukemia cell lines with the up- or down-regulation of TCF8 expression.** (A,B) The down-regulation of the TCF8 protein by *TCF8* siRNA. The CTLL2 (A) and MOLT4 (B) cell lines were transfected with either *TCF8* or the AllStars Negative Control (ANC) siRNAs and then were incubated for 24 hours. The levels of TCF8 protein were examined in each cell line by Western blotting (left panel). After transfection with siRNAs, the cells were treated with the indicated concentrations of TGF-β1 for 72 hours. The degree of proliferation of each cell line was examined by MTT assay. The results are shown as percentages of the values obtained from the control TGF-β1–free culture (right panel). A ◇ represents parental cells, □ represents cells treated with ANC siRNA, and ▲ represents cells treated with *TCF8* siRNA. Student *t* test ($P < .05$) was used for the statistical analysis. (C,D) The enforced expression of TCF8 in HTLV-1–infected cell lines. The TCF8 protein levels were examined in each MT-2 (C) and HUT102 (D) cell transfected with a mock or TCF8 expression plasmid after 24 hours by Western blotting (left panel). The cells were treated with the indicated concentrations of TGF-β1 for 72 hours and the proliferation of each was examined by MTT assay. The results are shown as percentages of the values obtained from the control TGF-β1–free culture (right panel). Parental cells (◇), mock vector-transfected cells (□), and TCF8 expression plasmid-transfected cells (▲). All data are the means plus or minus standard deviation in a duplicate assay. Student *t* test ($P < .05$) was used for the statistical analysis.

proteins to activate TGF-β1 signal transduction,[40,41] we investigated whether the down-regulation of TCF8 expression was associated with resistance to TGF-β1–mediated growth inhibition in ATLL cells. Thereafter, either *TCF8* or ANC siRNA was introduced into a murine IL2–dependent T-lymphoma cell line, CTLL2, and human T-ALL cell line, MOLT4. Western blot analyses revealed the TCF8 expression in the siRNA-treated cells to be less than half of that in the control cells, while the viable cell curves of both cell lines treated with *TCF8* siRNA exhibited a significantly higher resistance to TGF-β1 than those of the control cells (Figure 6A,B). Next, the TCF8 expression plasmid was transiently introduced into 2 HTLV-1–infected T-cell lines (MT2 and HUT102) and up to 40% of the TCF8 transfectants died after TGF-β1 treatment in a dose-dependent manner, whereas the parental and transfectants with mock plasmid did not die with TGF-β1 treatment at all (Figure 6C,D). These results indicate that down-regulation of TCF8 expression is one of the mechanisms of TGF-β1 resistance in ATLL cells, suggesting that $CD4^+$ T lymphoma cells might escape from negative selection due to reduced TGF-β1 responsiveness.

## Discussion

We demonstrated that in ATLL cells, the *TCF8* gene was mainly epigenetically inactivated in a majority of ATLL cells. In addition,

*TCF8* (or $\delta EF1^{\Delta C\text{-}fm}$ homozygous) mutant mice frequently developed CD4$^+$ T-cell lymphoma and/or leukemia after a few months. These findings indicate that *TCF8* has a tumor suppressor role in ATLL. Since the heterozygous *TCF8* mutant mice did not develop any tumors and the level of TCF8 expression in some ATLL cells was approximately 30% to 40% of that observed in the control CD4 lymphocytes, TCF8 may therefore be involved in only some and not all of ATLL development. On the other hand, it is reported that *TCF8* overexpressed in colorectal or breast cancer cells induces epithelial-mesenchymal transition (EMT) with the development of metastatic properties such as migration and invasion in vitro and in vivo.[42] Therefore, *TCF8* has dual functions in cancer progression, which are dependent on the type of the tumors, such as *WT1* or *TSLC1* tumor suppressor genes.[43,44]

It was previously reported that *TCF8* mutant mice had a defect in T-cell development in the first week of life.[28] At the early stage of development, intrathymic c-kit$^+$ T precursor cells in these mice were depleted to just 1% of the level in normal mice, and the number of CD8$^+$ SP T cells was significantly reduced relative to the number of CD4$^+$ SP T cells. These observations indicate that TCF8 is involved in the regulation of T-cell development at multiple stages. Lymphoma cells in *TCF8* mutant mice showed either CD4$^+$ SP T cells or DP T cells after 6 months. Interestingly, TGF-β1 was important for regulating T-cell development in the thymus and for negative selection at the late stage of differentiation of DP T cells to CD4$^+$ SP cells.[34] Recently, DNA microarray analysis identified a higher level of *TCF8* expression in DP thymocytes to CD4$^+$ SP T cells,[45] suggesting that TCF8 enhanced negative selection due to TGF-β1 responsiveness. Moreover, *TGF-β1*–deficient mice had an increased number of CD4$^+$ SP T cells and a decreased number of CD8$^+$ SP T cells.[46,47] By correlating the development of CD4$^+$ SP T-lymphoma cells in *TCF8* mutant mice with the increase in the number of CD4$^+$ T cells in *TGF-β1*–deficient mice, we concluded that leukemogenesis in *TCF8* mutant mice was partly dependent on resistance to TGF-β1.

TCF8 is an E-box–binding transcription factor reported to regulate many genes. We found that the transcription of *CD4*, *α4 integrin*, and *GATA-3*, which was reported to be suppressed by TCF8,[48] was up-regulated in ATLL cells (data not shown). It was therefore suggested that impaired regulation of TCF8 expression in ATLL induced the increase in expression of *CD4* and *GATA3*, which was crucial for the establishment of the ATLL phenotype in CD4$^+$ SP helper T lymphocytes. Moreover, TCF8 was reported to regulate p73, CCNG2, or p130.[49,50] Since these genes are very important for cell-cycle progression and apoptosis, further investigation is needed to determine which ones are directly related to leukemogenesis among those regulated by TCF8.

The phenotypes of T-cell lymphomas in *TCF8* mutant mice were very similar to those of ATLL patients. In *TCF8* mutant mice, the tumor cells were mainly CD4$^+$ SP or DP T cells, which invaded various organs, such as the liver, spleen, and lungs. In ATLL, the tumor cells were mainly CD4$^+$ SP T cells that also invaded various organs. One difference, however, was that thymic lymphomas developed in the *TCF8* mutant mice, which has not been reported in ATLL cases. Another difference is that lymphoma cells in *TCF8* mutant mice did not have multilobulated nuclei. Such nuclei result from alterations in the PI3-kinase signaling cascades,[51] suggesting that down-regulation of TCF8 expression is not related to the PTEN signaling pathway and that other mutations are necessary for the development of ATLL. This is the first report illustrating the importance of the disruption of *TCF8* in leukemogenesis of ATLL.

## Acknowledgments

We thank Drs M. Shiraga, I. Nishikata, and T. Uetsuki for technical assistance and advice on the paper.

This work was supported by Grants-in-Aid for Scientific Research of Priority Area and for 21st Century COE program (Life science) from the Ministry of Education, Culture, Sports, Science and Technology, Japan Leukemia Research fund, and Research fund from Miyazaki Prefecture Collaboration of Regional Entities for the Advancement of Technological Excellence, Japan Science and Technology Corporation.

## Authorship

Contribution: T.H., S.N., and K.H. designed and performed experiments, analyzed data, and drafted the paper; M.H. performed experiments; T.K., Y.A., T.T., K.N., and M.T. performed experiments and data analysis; Y.A. and R.Y. performed the histopathology; K.Y., A.O., and H.T. collected case material and supervised the project; J.Y. and Y.H. supervised the project and drafted the paper; K.M. designed the experiments, analyzed data, and drafted the paper.

Conflict-of-interest disclosure: The authors declare no competing financial interests.

Correspondence: Kazuhiro Morishita, Division of Tumor and Cellular Biochemistry, Department of Medical Sciences, Faculty of Medicine, University of Miyazaki, 5200 Kihara, Kiyotake, Miyazaki, Japan, 889-1692; e-mail: kmorishi@med.miyazaki-u.ac.jp.

## References

1. Takatsuki K, Yamaguchi K, Kawano F, et al. Clinical diversity in adult T-cell leukemia-lymphoma. Cancer Res. 1985;45:4644s-4645s.
2. Matsuoka M. Human T-cell leukemia virus type I and adult T-cell leukemia. Oncogene. 2003;22: 5131-5140.
3. Yoshida M. Multiple viral strategies of HTLV-1 for dysregulation of cell growth control. Annu Rev Immunol. 2001;19:475-496.
4. Tamiya S, Matsuoka M, Etoh K. Two types of defective human T-lymphotropic virus type I provirus in adult T-cell leukemia. Blood. 1996;88:3065-3073.
5. Koiwa T, Hamano-Usami A, Ishida T. 5'-long terminal repeat-selective CpG methylation of latent human T-cell leukemia virus type 1 provirus in vitro and in vivo. J Virol. 2002;76:9389-9397.
6. Okamoto T, Ohno Y, Tsugane S, et al. Multi-step carcinogenesis model for adult T-cell leukemia. Jpn J Cancer Res. 1989;80:191-195.
7. Look AT. Oncogenic transcription factors in the human acute leukemias. Science. 1997;278: 1059-1064.
8. Kamada N, Sakurai M, Miyamoto K, et al. Chromosome abnormalities in adult T-cell leukemia/lymphoma: a karyotype review committee report. Cancer Res. 1992;52:1481-1493.
9. Tsukasaki K, Krebs J, Nagai K, et al. Comparative genomic hybridization analysis in adult T-cell leukemia/lymphoma: correlation with clinical course. Blood. 2001;97:3875-3881.
10. Oshiro A, Tagawa H, Ohshima K, et al. Identification of subtype-specific genomic alterations in aggressive adult T-cell leukemia/lymphoma. Blood. 2006;107:4500-4507.
11. National Center for Biotechnology Information. GenBank. http://www.ncbi.nlm.nih.gov/site/entrez. Accessed December 12, 2007.
12. Williams TM, Moolten D, Burlein J, et al. Identification of a zinc finger protein that inhibits IL-2 gene expression. Science. 1991;25:1791-1794.
13. Barrallo-Gimeno A, Nieto MA. The Snail genes as inducers of cell movement and survival: implications in development and cancer. Development. 2005;132:3151-3161.
14. Thiery JP, Sleeman JP. Complex networks orchestrate epithelial-mesenchymal transitions. Nat Rev Mol Cell Biol. 2006;7:131-142.
15. Sasaki H, Nishikata I, Shiraga T, et al. Overexpression of a cell adhesion molecule, TSLC1, as

a possible molecular marker for acute-type adult T-cell leukemia. Blood. 2005;105:1204-1213.

16. Shimoyama M. Diagnostic criteria and classification of clinical subtypes of adult T-cell leukeamia-lymphoma: a report from the Lymphoma Study Group (1984-87). Br J Haematol. 1991;79:428-437.
17. Schneider U, Schwenk HU, Bornkamm G. Characterization of EBV-genome negative "null" and "T" cell lines derived from children with acute lymphoblastic leukemia and leukemic transformed non-Hodgkin lymphoma. Int J Cancer. 1977;19:621-626.
18. Minowada J, Onuma T, Moore GE. Rosette-forming human lymphoid cell lines. I. Establishment and evidence for origin of thymus-derived lymphocytes. J Natl Cancer Inst. 1972;49:891-895.
19. Yamada Y, Ohmoto Y, Hata T, et al. Features of the cytokines secreted by adult T cell leukemia (ATL) cells. Leuk Lymphoma. 1996;21:443-447.
20. Okada M, Maeda M, Tagaya Y, et al. TCGF (IL 2)-receptor induction Factor (S), II: possible role of ATL-derived factor (ADF) on constitutive IL 2 receptor expression of HTLV-1(+) T cell lines. J Immunol. 1985;135:3995-4003.
21. Miyoshi I, Kubonishi I, Yoshimoto S, et al. Type C virus particles in a cord T-cell line derived by cocultivating normal human cord leukocytes and human leukaemic T cells. Nature. 1981;294:770-771.
22. Gillis S, Smith KA. Long term culture of tumour-specific cytotoxic T cells. Nature. 1977;268:154-156.
23. Shaffer LG, Tommerup N (eds). ISCN (2005): An International System for Human Cytogenetic Nomenclature. S. Karger, Basel; 2005.
24. Kakazu N, Taniwaki M, Horiike S, et al. Combined spectral karyotyping and DAPI banding analysis of chromosome abnormalities in myelodysplastic syndrome. Gene Chromosome Cancer. 1999;26:336-345.
25. Taniwaki M, Nishida K, Ueda Y, et al. Interphase and metaphase detection of the breakpoint of 14q32 translocations in B-cell malignancies by double-color fluorescence in situ hybridization. Blood. 1995;85:3223-3228.
26. National Center for Biotechnology Information. http://www.ncbi.nlm.nih.gov/project/genome. Accessed December 12, 2007.
27. Nannya Y, Sanada M, Nakazaki K, et al. A robust algorithm for copy number detection using high-density oligonucleotide single nucleotide polymorphism genotyping arrays. Cancer Res. 2005;65:6071-6079.
28. Higashi Y, Moribe H, Takagi T, et al. Impairment of T cell development in deltaEF1 mutant mice. J Exp Med. 1997;185:1467-1479.
29. Takagi T, Moribe H, Kondoh H, Higashi Y. DeltaEF1, a zinc finger and homeodomain transcription factor, is required for skeleton patterning in multiple lineages. Development. 1998;125:21-31.
30. Hark AT, Schoenherr CJ, Katz DJ, et al. CTCF mediates methylation-sensitive enhancer-blocking activity at the H19/Igf2 locus. Nature. 2000;405:486-489.
31. Bell AC, Felsenfeld G. Methylation of a CTCF-dependent boundary controls imprinted expression of the Igf2 gene. Nature. 2000;405:482-485.
32. Schmelz K, Wagner M, Dörken B, Tamm I. 5-Aza-2′-deoxycytidine induces p21WAF expression by demethylation of p73 leading to p53-independent apoptosis in myeloid leukemia. Int J Cancer. 2005;114:683-695.
33. Soengas MS, Capodieci P, Polsky D. Inactivation of the apoptosis effector Apaf-1 in malignant melanoma. Nature. 2001;409:207-211.
34. Licona-Limon P, Soldevila G. The role of TGF-beta superfamily during T cell development: new insights. Immunol Lett. 2007;109:1-12.
35. Niitsu Y, Urushizaki Y, Koshida Y, et al. Expression of TGF-beta gene in adult T cell leukemia. Blood. 1988;71:263-266.
36. Kim SJ, Kehrl JH, Burton J, et al. Transactivation of the transforming growth factor beta 1 (TGF-beta 1) gene by human T lymphotropic virus type 1 tax: a potential mechanism for the increased production of TGF-beta 1 in adult T cell leukemia. J Exp Med. 1990;172:121-129.
37. Yoshida M, Nosaka K, Yasunaga J, Nishikata I, Morishita K, Matsuoka M. Aberrant expression of the MEL1S gene identified in association with hypomethylation in adult T-cell leukemia cells. Blood. 2004;103:2753-2760.
38. Arnulf B, Villemain A, Nicot C, et al. Human T-cell lymphotropic virus oncoprotein Tax represses TGF-beta 1 signaling in human T cells via c-Jun activation: a potential mechanism of HTLV-I leukemogenesis. Blood. 2002;100:4129-4138.
39. Xu X, Heidenreich O, Kitajima I, et al. Constitutively activated JNK is associated with HTLV-1 mediated tumorigenesis. Oncogene. 1996;13:135-142.
40. Postigo AA. Opposing functions of ZEB proteins in the regulation of the TGFβ/BMP signaling pathway. EMBO J. 2003;22:2443-2452.
41. Postigo AA, Depp JL, Taylor JJ, Kroll KL. Regulation of Smad signaling through a differential recruitment of coactivators and corepressors by ZEB proteins. EMBO J. 2003;22:2453-2462.
42. Peinado H, Olmeda D, Cano A. Snail, Zeb and bHLH factors in tumour progression: an alliance against the epithelial phenotype? Nat Rev Cancer. 2007;7:415-428.
43. Murakami Y. Involvement of a cell adhesion molecule, TSLC1/IGSF4, in human oncogenesis. Cancer Sci. 2005;96:543-552.
44. Yang L, Han Y, Saurez Saiz F, Minden MD. A tumor suppressor and oncogene: the WT1 story. Leukemia. 2007;21:868-876.
45. Dik WA, Pike-Overzet K, Weerkamp F, et al. New insights on human T cell develoment by quantitative T cell receptor gene rearrangement studies and gene expression profiling. J Exp Med. 2005;201:1715-1723.
46. Christ M, McCartney-Francis NL, Kulkarni AB, et al. Immune dysregulation in TGF-β1-deficient mice. J Immunol. 1994;153:1936-1946.
47. Plum J, De Smedt M, Leclercq G, Vandekerckhove B. Influence of TGF-β on murine thymocyte development in fetal thymus organ culture. J Immunol. 1995;154:5789-5798.
48. Postigo AA, Dean DC. Independent repressor domains in ZEB regulate muscle and T-cell differentiation. Mol Cell Biol. 1999;19:7961-7971.
49. Fontemaggi G, Gurtner A, Damalas A, et al. δEF1 repressor controls selectively p53 family members during differentiation. Oncogene. 2005;24:7273-7280.
50. Chen J, Yusuf I, Andersen HM, Fruman DA. FOXO transcription factors cooperate with δEF1 to activate growth suppressive genes in B lymphocytes. J Immunol. 2006;176:2711-2721.
51. Fukuda R, Hayashi A, Utsunomiya A, et al. Alteration of phosphatidylinositol 3-kinase cascade in the multilobulated nuclear formation of adult T cell leukemia/lymphoma (ATLL). Proc Natl Acad Sci U S A. 2005;102:15213-15218.

# Novel gain-of-function mutation in the extracellular domain of the *PDGFRA* gene in infant acute lymphoblastic leukemia with t(4;11)(q21;q23)

*Leukemia* (2008) **22**, 2279–2280; doi:10.1038/leu.2008.140; published online 12 June 2008

Platelet-derived growth factor receptors α and β (PDGFRA and PDGFRB) belong to the class III receptor tyrosine kinases, which include c-KIT, colony stimulating factor-1 receptor and FLT3.[1] *PDGFRA* and *c-KIT* are two related receptor tyrosine kinases showing similar structure, and mutations of these genes are detected in gastrointestinal stromal tumor[2,3] and myeloproliferative disorders.[4] Recently, we reported a *PDGFRA* N870S mutation in a 13-year-old boy having acute myelogenous leukemia (AML)-M1 with t(8;21) and an F808L mutation in a 13-year-old girl having AML-M1 with inv(16).[5] In addition to point mutations, the *FIP1L1-PDGFRA* fusion tyrosine kinase resulting from internal deletion of 4q12 locus was described in a subgroup of patients presenting hypereosinophilic syndrome.[6] Here, we investigated whether *PDGFRA* is also implicated in the pathogenesis of acute lymphoblastic leukemia (ALL), and found a mutation which renders a factor-dependent cell line factor-independent by its aberrant tyrosine phosphorylation.

One hundred and twenty seven childhood ALL and 40 infant ALL samples, including those from 13 patients with t(4;11)(q21;q23) (one patient was childhood ALL and the others were infant ALL), were analyzed for the expression and mutation of *PDGFRA*. *PDGFRA* gene was expressed in 38 (29.9%) of the 127 childhood ALL patient samples, 12 (30.0%) of the 40 infant ALL patients and 9 (36.0%) of the 25 ALL patients associated with *MLL* gene rearrangements. Sequence analyses of the samples expressing *PDGFRA* revealed a *PDGFRA* A509D mutation (Figure 1a) in a 4-month-old boy having ALL with t(4;11)(q21;q23). This mutation in the Ig5 domain of *PDGFRA* corresponds to those responsible for ligand-independent kinase activation of *c-KIT* in gastrointestinal stromal tumor.[3] Mutations on exon 9 encoding the extracellular domain near the transmembrane domain of *c-KIT* lead to ligand-independent activation of c-KIT,[2,3] and are associated with core binding factor AML and gastrointestinal stromal tumor.[1,3,7] We examined whether the mutation at Ig5 domain of the *PDGFRA* gene resulted in constitutive activation of the kinase activity by retroviral transduction[8] of the wild-type and mutated *PDGFRA* cDNAs into an IL-3 dependent mouse cell line, Ba/F3 and stable cell lines expressing each transgene were established. The whole coding region of *PDGFRA* cDNA was sequenced directly or after subcloning into a retroviral vector pMXs-IN(IRES-Neo).[8] The empty vector as a negative control was also introduced into Ba/F3 cells. As expected, the wild-type PDGFRA was not significantly phosphorylated on tyrosine residues in the absence of PDGF (Figure 1b). In contrast, the PDGFRA with the Ig5 domain A509D mutation was phosphorylated in the absence of PDGF (Figure 1b). Because the signal transduction pathway of PDGFRA is comparable with that of c-KIT,[2] the gain-of-function mutations of PDGFRA by themselves may transform Ba/F3 cells. In fact, Ba/F3 cells expressing the A509D mutant PDGFRA grew in the absence of IL-3 and PDGF whereas those expressing the wild-type did not (data not shown). It is possible that the mutant PDGFRA may contribute to leukemogenesis with t(4;11).

In conclusion, we reported the frequency of *PDGFRA* mutations in a large series of Japanese pediatric and infantile ALL patients. This is the first report showing a constitutively active *PDGFRA* mutation found in an ALL patient that may be associated with leukemic cell growth.

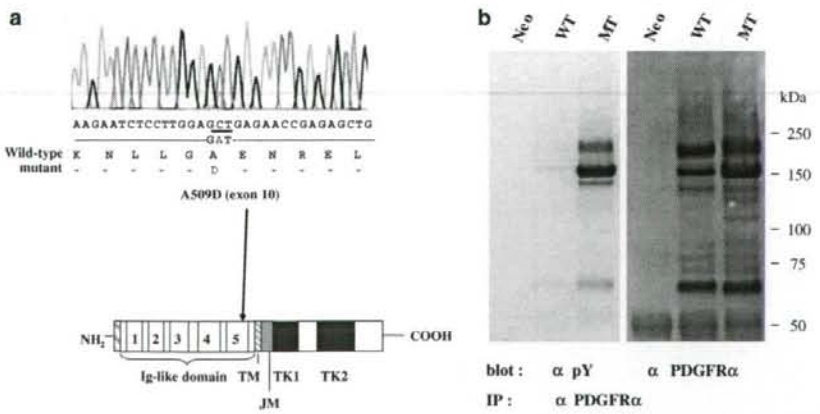


**Figure 1** cDNA sequencing and position of the mutation of the *platelet-derived growth factor receptor α* (*PDGFRA*) gene at the Ig5 domain and tyrosine phosphorylation of the PDGFRA mutant. (**a**) Direct sequencing of the PCR product for the *PDGFRA* from an ALL patient with t(4;11) demonstrates the wild-type (WT) (top), and the A509D mutant (bottom) alleles. (**b**) Functional analysis of the WT PDGFRA and the A509D mutant derived from an ALL with t(4:11) patient. The mutant (MT), but not the WT PDGFRA was phosphorylated on tyrosine residues in Ba/F3 cells after retroviral transduction. Ba/F3 cells transduced with the empty vector (Neo) and those with the WT expressor were cultured with IL-3, and those with the MT expressor were cultured without IL-3. Lysates were prepared from cultured cells, immunoprecipitated with a polyclonal antibody to PDGFRA (sc-338, Santa Cruz Biotechnology, Santa Cruz, CA, USA), and immunoblotted with an anti-phosphotyrosine (pY) monoclonal antibody (Upstate Biotechnology, Inc., Lake Placid, NY, USA) (left panel), and with the anti-PDGFRA antibody (sc-338) (right panel). There was no detectable phosphorylation of WT PDGFRA. IP, immunoprecipitation. Ig, immunoglobulin; TM, transmembrane domain; JM, juxtamembrane domain; TK1 and TK2, two intracellular kinase domains.

**Acknowledgements**

We thank S Sohma and H Soga for technical assistance. We also thank Dr S Hirota for wild-type PDGFRA expression plasmid. This work was supported by a Grant-in-Aid for Cancer Research from the Ministry of Health, Labor, and Welfare of Japan, a Grant-in-Aid for Scientific Research on Priority Areas, and Grants-in-Aid from the Ministry of Education, Culture, Sports, Science and Technology of Japan.

M Hiwatari[1,4], R Ono[2,4], T Taki[3], A Hishiya[4], E Ishii[5], T Kitamura[4], Y Hayashi[6] and T Nosaka[2,4]

[1]*Department of Pediatrics, Graduate School of Medicine, The University of Tokyo, Tokyo, Japan;*
[2]*Department of Microbiology, Mie University Graduate School of Medicine, Tsu, Japan;*
[3]*Department of Molecular Laboratory Medicine, Kyoto Prefectural University of Medicine Graduate School of Medical Science, Kyoto, Japan;*
[4]*Division of Cellular Therapy, The Institute of Medical Science, The University of Tokyo, Tokyo, Japan;*
[5]*Department of Pediatrics, Ehime University Graduate School of Medicine, Ehime, Japan and*
[6]*Gunma Children's Medical Center, Gunma, Japan*
*E-mail: nosaka@doc.medic.mie-u.ac.jp or hayashiy-tky@umin.ac.jp*

**References**

1 Blume-Jensen P, Hunter T. Oncogenic kinase signalling. *Nature* 2001; **411**: 355–365.
2 Fletcher JA. Role of KIT and Platelet-Derived Growth Factor Receptors as Oncoproteins. *Seminars in Oncology* 2004; **31**: 4–11.
3 Hirota S, Nishida T, Isozaki K, Taniguchi M, Nakamura J, Okazaki T *et al.* Gain-of-function mutation at the extracellular domain of KIT in gastrointestinal stromal tumours. *Journal of Pathology* 2001; **193**: 505–510.
4 Tefferi1 A, Gilliland DG. Oncogenes in Myeloproliferative Disorders. *Cell Cycle* 2007; **5**: 550–566.
5 Hiwatari M, Taki T, Tsuchida M, Hanada R, Hongo T, Sako M *et al.* Novel missense mutations in the tyrosine kinase domain of the platelet-derived growth factor receptor alpha(PDGFRA) gene in childhood acute myeloid leukemia with t(8;21)(q22;q22) or inv(16)(p13q22). *Leukemia* 2005; **19**: 476–477.
6 Burgstaller S, Kreil S, Waghorn K, Metzgeroth G, Preudhomme C, Zoi K *et al.* The severity of *FIP1L1–PDGFRA*-positive chronic eosinophilic leukaemia is associated with polymorphic variation at the *IL5RA* locus. *Leukemia* 2007; **21**: 2428–2432.
7 Wang YY, Zhou GB, Yin T, Chen B, Shi JY, Liang WX *et al. AML1–ETO* and *C-KIT* mutation/overexpression in t(8;21) leukemia: Implication in stepwise leukemogenesis and response to Gleevec. *Proc Natl Acad Sci USA* 2005; **102**: 1104–1109.
8 Kitamura T, Koshino Y, Shibata F, Oki T, Nakajima H, Nosaka T *et al.* Retrovirus-mediated gene transfer and expression cloning: Powerful tools in functional genomics. *Exp Hematol* 2003; **31**: 1007–1014.

# Clinical and biological significance of *RAS* mutations in multiple myeloma

*Leukemia* (2008) **22**, 2280–2284; doi:10.1038/leu.2008.142; published online 5 June 2008

Primary genetic abnormalities in myeloma (MM) such as trisomies of chromosomes 3, 5, 7, 9, 11, 15, 19 and 21 associated with hyperdiploid MM and translocations involving the immunoglobulin heavy chain (IgH) locus on chromosome 14q32 and three main recurrent partners: MMSET/FGFR3, CCND1 and c-MAF are already present in the pre-malignant monoclonal gammopathy of undetermined significance (MGUS) stage.[1] Some patients with these genetic abnormalities may remain as MGUS for many years without transforming to MM, suggesting that they are involved in clonal initiation but do not mediate malignant transformation.

One of the recurrent differences between MGUS and MM is the presence of *RAS* mutations in the latter. *RAS* mutations may, therefore, play an important role in malignant transformation of clonal plasma cells and myeloma pathogenesis. However, the clinical and biological significance of *RAS* mutation in MM has not been clearly established as most of the previous studies have involved small numbers of heterogeneously treated patients.

To establish the clinical and biological significance of *RAS* mutation in MM, we studied the association of *RAS* mutation with a comprehensive spectrum of clinical parameters including the newly established ISS staging and survival, as well as a panel of known recurrent genetic abnormalities in MM such as t(4;14), t(14;16), t(11;14), chromosome 13 and 17p13 deletion detected by fluorescent *in situ* hybridization[2] and ploidy assessed by DNA content measurement using flow cytometry,[3] in a large cohort of newly diagnosed patients enrolled in the Eastern Cooperative Group (ECOG) clinical trial E9486/E9487 ($N=561$).[4] A total of 439 patients, based on sample availability, were included (The ECOG Cohort). For this cohort, DNA from unsorted whole bone marrow was used for *RAS* mutation studies. We also studied 14 MGUS patients and 82 MM patients (60 newly diagnosed and 22 relapsed) from the Mayo Clinic (Mayo Cohort). Bone marrow samples were obtained after informed consent according to the Declaration of Helsinki. The study was approved by the Mayo Clinic Institution Review Board. CD138 positive plasma cells were enriched using immuno-magnetic beads (AutoMACS; Miltenyi-Biotec, Auburn, CA, USA). RNA and DNA from these enriched cells were used for gene expression and *RAS* mutation studies, respectively.

Conformation sensitive gel electrophoresis was used to screen samples for *KRAS* (codons 12, 13 and 61) and *NRAS* (codons 12, 13 and 61) mutations (Supplementary Methods). *RAS* mutation was detected in 102 (23%) patients in the ECOG cohort. Seventy-four (17%) patients had mutations in *NRAS*. The majority of these mutations were in codon 61 (64 of the 74), with 5 mutations detected in codons 12 and 13. We also found mutations in codon 64 ($n=1$) and codon 86 ($n=4$). Twenty-eight (6%) patients had mutations in K-*RAS*. Twenty-two of these are in codons 12 and 13 and three in codon 61. In addition, we also found one mutation each in codon 16, 22 and 24. In the Mayo Clinic cohort, *RAS* mutation was detected in 1 of 14 MGUS patients (7%), 15 of 60 newly diagnosed MM patients (25%) and 10 of 22 relapsed MM patients (45%). Once again N-*RAS* mutations were more common that K-*RAS* mutations. Our study confirms the low incidence of *RAS* mutation in MGUS compared to MM found in a previous study,[5] consistent with

ELSEVIER

Cancer Genetics and Cytogenetics 186 (2008) 115–119

CANCER GENETICS AND CYTOGENETICS

Short communication

# *MNX1–ETV6* fusion gene in an acute megakaryoblastic leukemia and expression of the *MNX1* gene in leukemia and normal B cell lines

Takeshi Taketani[a,b], Tomohiko Taki[c], Masahiro Sako[d], Takefumi Ishii[d], Seiji Yamaguchi[a], Yasuhide Hayashi[e,*]

[a]*Department of Pediatrics, Shimane University Faculty of Medicine, Izumo, Shimane, Japan*
[b]*Division of Blood Transfusion, Shimane University Hospital, Matsue, Shimane, Japan*
[c]*Department of Molecular Laboratory Medicine, Kyoto Prefectural University of Medicine Graduate School of Medical Science, Kyoto, Japan*
[d]*Department of Pediatric Hematology/Oncology, Osaka City General Hospital, Osaka, Japan*
[e]*Department of Hematology/Oncology, Gunma Children's Medical Center, 779 Shimohakoda, Hokkitsu, Shibukawa, Gunma 377-8577, Japan*

Received 5 March 2008; received in revised form 11 June 2008; accepted 27 June 2008

**Abstract** Patients with infant acute myeloid leukemia (AML) who carry a t(7;12)(q36;p13) translocation have been reported to have a poor clinical outcome. *MNX1–ETV6* fusion transcripts (previously *HLXB9–ETV6*) were rarely detected in AML patients having t(7;12)(q36;p13). A 23-month-old girl with acute megakaryoblastic leukemia (AMKL) exhibited chromosome abnormalities, including add(7)(q22), and del(12)(p12p13). Southern blot analysis of bone marrow cells showed an *ETV6* gene rearrangement. Reverse transcriptase-polymerase chain reaction (RT-PCR) followed by sequence analysis revealed the presence of an *MNX1–ETV6* fusion gene. The patient responded well to chemotherapy, achieved complete remission, and at writing had been in complete remission for 60 months. The *MNX1* expression by RT-PCR was significantly more frequent in Epstein–Barr virus–transformed B-cell lines derived from normal adult lymphocytes than in leukemic cell lines. This represents a novel case of an AMKL patient with *MNX1–ETV6* fusion transcripts who had a good prognosis. 

## 1. Introduction

Many recurrent chromosomal translocations are involved in acute myeloid leukemia (AML) [1]. AML with 12p13 translocations have been reported to involve the ETS variant gene 6 (*TEL* oncogene) (*ETV6*) [2]. In cases of AML carrying 12p13 abnormalities, a recurrent translocation t(7;12)(q36;p13) is found in 20%–30% of infant cases [3–5]. Fluorescence in situ hybridization assay is needed to evaluate this translocation, because it is difficult to detect by conventional karyotyping [3–5]. AML patients with this translocation are characterized by age under 20 months at diagnosis, thrombocytosis, high percentage of CD34-positive cells, presence of additional chromosomal abnormalities, including trisomy 19 or trisomy 8 (or both), and a poor prognosis [3–5]. An *MNX1–ETV6* fusion gene (previously *HLXB9–ETV6*) was identified in two pediatric AML patients having t(7;12)(q36;p13) [6]; however, heterogeneity of the 7q36 and 12p13 translocations was reported [5,7,8]. Thus, *MNX1–ETV6* fusion gene in AML patients having t(7;12) is infrequently reported [7,8].

We describe the case of a 23-month-old AML patient with add(7)(q22), del(12)(p12p13), and *MNX1–ETV6* fusion transcript; the child has remained alive for 5 years. We also report the expression of the *MNX1* gene in several leukemic and normal Epstein–Barr virus-transformed cell lines.

## 2. Case report

A 23-month-old girl was admitted to Osaka City General Hospital because of appetite loss and pallor. Blood examination showed a white blood cell count of 10,520/μL with 55.5% blasts, a hemoglobin level of 7.0 g/dL, and a platelet count of 164,000/μL. She had a mediastinal mass, but no hepatosplenomegaly. Bone marrow examination revealed a nuclear cell count of 30,000/μL with 71.2% blasts. The

* Corresponding author. Tel.: +81-279-52-3551, ext. 2200; fax: +81-279-52-2045.
*E-mail address:* hayashiy-tky@umin.ac.jp (Y. Hayashi).

0165-4608/08/$ – see front matter 
doi:10.1016/j.cancergencyto.2008.06.009

blasts were negative for myeloperoxidase staining and platelet peroxidase staining electron-microscopically. Flow cytometric analysis showed that the blasts expressed CD41, CD36, CD13, CD33, CD15, and CD7 antigens, suggesting megakaryoblastic origin. Conventional G-banding chromosomal analysis revealed a karyotype of 46,XX,add (7)(q22),del(12)(p12p13) in all 20 bone marrow cells examined (Fig. 1).

The patient was diagnosed as having AMKL (M7 subtype, based on the French–American–British classification), and was treated on the Japanese Childhood AML Cooperative Study Group Protocol, AML99 [9]. She obtained complete remission with induction chemotherapy (cytarabine, etoposide, and mitoxantrone). Thereafter, she was treated with five additional courses of intensive chemotherapy (high-dose cytarabine, etoposide, idarubicin, and mitoxantrone). As of writing, she had been in complete remission for 60 months after diagnosis.

## 3. Materials and methods

### *3.1. Southern blot analysis*

High molecular weight DNA was extracted from bone marrow cells of the patient by proteinase K digestion and phenol–chloroform extraction [10]. Ten micrograms of DNA was digested with *Eco*RI, subjected to electrophoresis on 0.7% agarose gels, and transferred to nylon membrane, and hybridized to cDNA probes $^{32}$P-labeled by the random hexamer method [10]. The probes used were a 516-bp *MNX1* cDNA fragment (nucleotide nt598 to nt1114; GenBank accession no. NM_005515; previously *HLXB9*).

### *3.2. Expression of WT1 mRNA and mutation of FLT3*

*WT1* mRNA was examined for detection of minimal residual disease as previously reported [11]. Internal tandem duplication and mutation of *FLT3* were examined as previously reported [10].

### *3.3. Reverse transcriptase–polymerase chain reaction and nucleotide sequencing*

*MNX1–ETV6* chimeric mRNA was detected by reverse transcriptase–polymerase chain reaction (RT-PCR) as described previously [12]. Total RNA was extracted from the leukemic cells of the patient using the acid guanidine thiocyanate–phenol chloroform method [12]. Total RNA (4 μg) was reverse-transcribed to cDNA, using a cDNA synthesis kit (GE Healthcare Bio-Science, Piscataway, NJ) [12]. PCR was performed with AmpliTaq Gold DNA polymerase (Applied Biosystems, Foster City, CA; Tokyo, Japan), using the reagents recommended by the manufacturer. The primers used and PCR conditions were as described previously [6]. The PCR products were subcloned into pCR2.1 vector (Invitrogen, Carlsbad, CA) and sequenced by the fluorometric method using the BigDye Terminator cycle sequencing kit (Applied Biosystems).

### *3.4. Expression of the MNX1 gene by RT-PCR in leukemic cell lines*

To analyze the expression pattern of the *MNX1* gene in leukemic cell lines, RT-PCR was performed. Fifty-nine cell lines were examined, as follows [12]; 10 B-precursor ALL cell lines (LC4-1, NALM-6, NALM-24, NALM-26, UTP-2, RS4;11, SCMC-L10, KOCL-33, KOCL-45, KOCL-69), 9

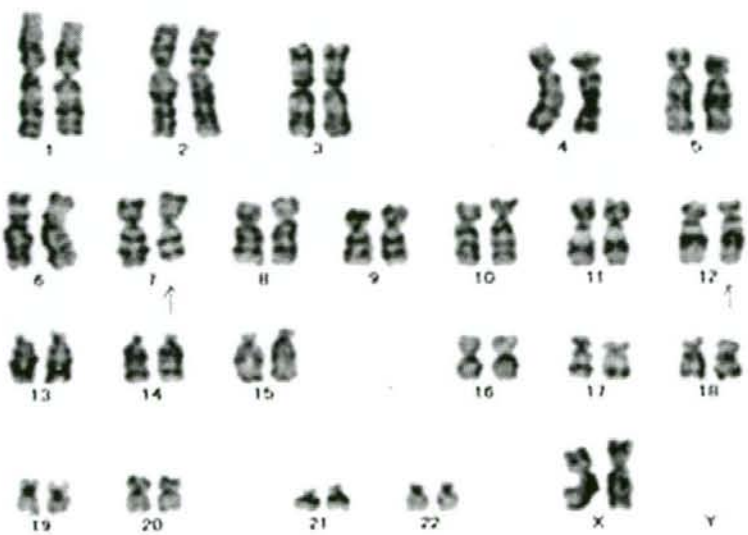


Fig. 1. G-banding karyotype of the leukemic cells in a pediatric patient with acute megakaryoblastic leukemia: 46,XX,add(7)(q22),del(12)(p12p13).

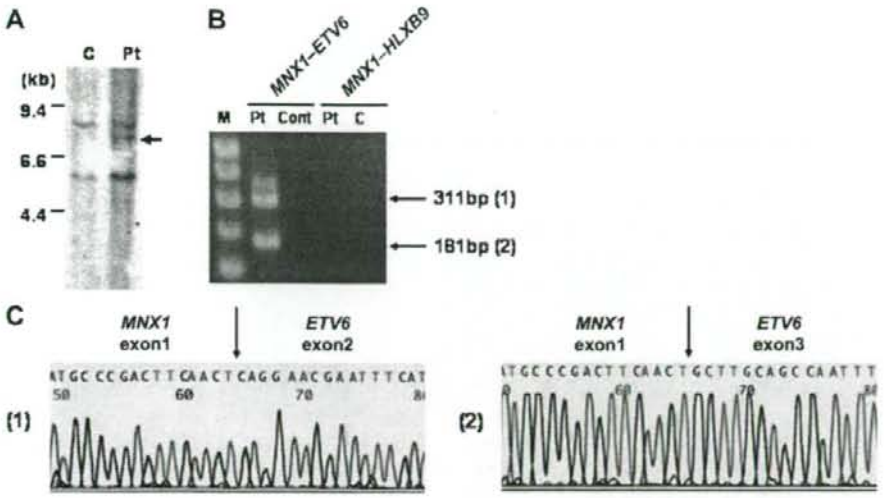


Fig. 2. Detection of the *MNX1–ETV6* fusion gene (previously *HLXB9–ETV6*). (A) Rearrangement of the *MNX1* gene by Southern blotting with *Eco*RI digestion. The arrow indicates a rearranged band of the *MNX1* gene; C, control; Pt, patient. (B) The *MNX1–ETV6* fusion transcript identified by reverse transcriptase–polymerase chain reaction (RT-PCR). Lanes 2 and 3, *MNX1–ETV6* fusion transcript; lanes 4 and 5, *ETV6–MNX1* fusion transcript. C, control; M, size marker; Pt, patient; (C) Nucleotide and amino acid sequencing of two *MNX1–ETV6* fusion transcripts.

B-ALL cell lines (BALM-1, BALM-13, BALM-14, BJAB, DAUDI, RAJI, RAMOS, BAL-KH, NAMALLA), 9 T-ALL cell lines (RPMI-8402, MOLT-14, THP-6, PEER, H-SB2, HPB-ALL, L-SAK, L-SMY, KCMC-T), 8 AML cell lines (YNH-1, ML-1, KASUMI-3, KG-1, inv-3, SN-1, NB4, HEL), 6 acute monocytic leukemia cell lines (THP-1, IMS/M1, CTS, P31/FUJ, MOLM-13, KOCL-48), 5 chronic myelogenous leukemia cell lines (MOLM-1, MOLM-7, TS9;22, SS9;22, K-562), 2 acute megakaryoblastic leukemia cell lines (CMS, CMY), and 10 Epstein-Barr virus transformed B lymphocyte (EBV-B) cell lines derived from normal adult peripheral lymphocytes. Five normal BM samples were also examined. RT-PCR mixtures and conditions were the same as described [10]. The primers used for RT-PCR were HLXB9-658F (5′-GGCATGATCCTGCCTAAGAT-3′) (sense primer) and HLXB9-1092R (TGCT GTAGGGGAAATGGTCGTCG) (antisense primer) [6].

## 4. Results and discussion

The karyotype of the patient's leukemic cells was 46,XX,add(7)(q22),del(12)(p12p13), suggesting that both *ETV6* and *MNX1* were involved in this chromosomal abnormality. With informed consent from the patient's parents, DNA and total RNA were extracted from bone marrow cells of the patient. Southern blot analysis of DNA from leukemic cells of the patient using the *MNX1* probe showed a rearranged band (Fig. 2A). We performed RT-PCR for *MNX1–ETV6* chimeric mRNA and obtained two RT-PCR products, of 311 bp and 181 bp (Fig. 2B). Sequence analysis of these PCR products showed that one product was an in-frame fusion transcript of exon 1 of *MNX1* to exon 3 of *ETV6*, and the other was an out-of-frame fusion transcript of exon 1 of *MNX1* to exon 2 of *ETV6* (Fig. 2C). These transcripts were the same as previously reported [6]. The reciprocal *ETV6–MNX1* transcript was not detected (Fig. 2B).

The *WT1* mRNA level was 3,400 copies/μg RNA at diagnosis, but decreased to <50 copies/μg RNA after remission. Neither internal tandem duplication nor mutation of *FLT3* were found in this patient, suggesting that the prognosis is not poor [1].

Table 1
Expression of the *MNX1* gene in leukemia and EBV-B cell lines by reverse transcriptase–polymerase chain reaction

| Cell line | Cells examined, no. | Cells expressing *MNX1*, no. (%) |
|---|---|---|
| ALL | 28 | 5 (17.9) |
| B precursor | 10 | 0 (0) |
| B | 9 | 2 (22.2) |
| T | 9 | 3 (33.3) |
| AML | 16 | 3 (18.8) |
| AML | 8 | 1 (12.5) |
| AMoL | 6 | 2 (33.3) |
| AMKL | 2 | 0 (0) |
| CML | 5 | 1 (20) |
| EBV-B | 10 | 7 (70) |
| normal BM | 5 | 0 (0) |

*Abbreviations:* ALL, acute lymphoblastic leukemia; AMKL, acute megakaryoblastic leukemia; AML, acute myeloid leukemia; AMoL, acute monocytic leukemia; B, B-cell; BM, bone marrow; CML, chronic myelogenous leukemia; EBV-B, Epstein–Barr virus-transformed human B lymphocytes; T, T-cell.

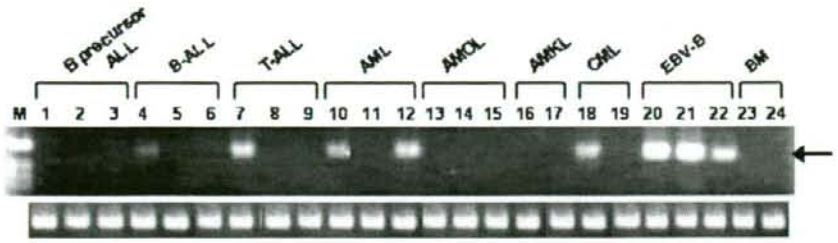


Fig. 3. Expression of the *MNX1* gene in leukemia and EBV-B cell lines by RT-PCR. ALL, acute lymphoblastic leukemia; AMKL, acute megakaryoblastic leukemia; AML, acute myeloid leukemia; AMOL, acute monocytic leukemia; B, B-cell; BM, bone marrow; CML, chronic myelogenous leukemia; EBV-B, Epstein–Barr virus-transformed human B lymphocytes; T, T-cell.

We next examined the *MNX1* expression by RT-PCR analysis in 49 leukemic cell lines, and 10 EBV-B cell lines. *MNX1* was not frequently expressed in lymphoid or myeloid leukemic cell lines (Table 1; Fig. 3). *MNX1* was expressed in 7 of 10 EBV-B cell lines, but not in 5 normal BM cells. The *MNX1* expression was significantly more frequent in EBV-B cell lines than in leukemic cell lines ($P = 0.0015$) or in normal BM cells ($P = 0.0256$). The *MNX1* was frequently expressed in CD34-positive cells purified from normal BM cells, acute leukemia cells, and AML cells having t(7;12)(q36;p13) [5,13,14]. It is unknown whether the incidence of *MNX1* expression differs among leukemia cell lines. Mature B-lineage cells are likely to frequently express *MNX1* transcripts, and the transcripts were more prevalent in several human B lineage cell line and tonsil B cells [15]. The present findings are compatible with previous reports. *MNX1* may be associated with differentiation of B cells.

*MNX1–ETV6* fusion transcript has so far been detected in only four out of the many AML patients who carry the t(7;12) anomaly [5,6]. Difficulty of detection of this fusion transcript is due to breakpoint heterogeneity of the 7q36 and 12p13 in this translocation [7,8]. Clinical features of AML patients having t(7;12) did not differ between the presence and absence of *MNX1–ETV6* fusion transcripts [5]. Notably, clinical characteristics of the present patient were different from those of AML patients having t(7;12) previously reported. Our patient was diagnosed as having AMKL, although most AML patients having t(7;12) were identified as poorly differentiated FAB subtypes [5]. Only one patient was reported to be diagnosed with AMKL; however, *MNX1–ETV6* fusion transcript was not examined in that case [4]. An additional cytogenetic abnormality is trisomy 19 [3–5]. Chromosomal analysis of the present patient showed absence of additional chromosomal abnormalities, suggesting long-term disease-free survival with chemotherapy alone. All AML patients, except one who had both t(7;12) and trisomy 19, died [3–6]. These findings suggest that t(7;12) is associated only with leukemogenesis, and that other factors including trisomy 19 and *FLT3* mutations, may affect the prognosis of AML patients having t(7;12).

In conclusion, an AMKL patient with *MNX1–ETV6* fusion transcripts had a good prognosis. Further accumulation of clinical and molecular data of AML patients having t(7;12) is needed to clarify this result.

## Acknowledgments

We express our appreciation to Mrs. Shoko Sohma and Hisae Soga for their excellent technical assistance. We thank Dr. Takeyuki Sato, Department of Pediatrics, Chiba University School of Medicine, Japan, for providing AMKL (CMS, CMY) cell lines; Dr. Kanji Sugita, Department of Pediatrics, Yamanashi University School of Medicine, Japan, for providing ALL (KOCL-33, -45, -69) cell lines and AMoL (KOCL-48) cell lines; and Dr. Yoshinobu Matsuo, Hayashibara Biochemical Laboratories, Inc., Fujisaki Cell Center, Japan, for providing varieties of ALL cell lines. This work was supported by a Grant-in-Aid for Cancer Research, Research on Children and Families from the Ministry of Health, Labor, and Welfare of Japan, a Grant-in-Aid for Scientific Research (C), and Exploratory Research from the Ministry of Education, Culture, Sports, Science, and Technology of Japan.

## References

[1] Hayashi Y. The molecular genetics of recurring chromosome abnormalities in acute myeloid leukemia. Semin Hematol 2000;37:368–80.

[2] Bohlander SK. *ETV6*: a versatile player in leukemogenesis. Semin Cancer Biol 2005;15:162–74.

[3] Tosi S, Harbott J, Teigler-Schlegel A, Haas OA, Pirc-Danoewinata H, Harrison CJ, Biondi A, Cazzaniga G, Kempski H, Scherer SW, Kearney L. t(7;12)(q36;p13), a new recurrent translocation involving *ETV6* in infant leukemia. Genes Chromosomes Cancer 2000;29:325–32.

[4] Slater RM, von Drunen E, Kroes WG, Weghuis DO, van den Berg E, Smit EM, van der Does-van den Berg A, van Wering E, Hählen K, Carroll AJ, Raimondi SC, Beverloo HB. t(7;12)(q36;p13) and t(7;12)(q32;p13): translocations involving *ETV6* in children 18 months of age or younger with myeloid disorders. Leukemia 2001;15:915–20.

[5] von Bergh AR, van Drunen E, van Wering ER, van Zutven LJ, Hainmann I, Lönnerholm G, Meijerink JP, Pieters R, Beverloo HB.

High incidence of t(7;12)(q36;p13) in infant AML but not in infant ALL, with a dismal outcome and ectopic expression of *HLXB9*. Genes Chromosomes Cancer 2006;45:731–9.

[6] Beverloo HB, Panagopoulos I, Isaksson M, van Wering E, van Drunen E, de Klein A, Johansson B, Slater R. Fusion of the homeobox gene *HLXB9* and the *ETV6* gene in infant acute myeloid leukemias with the t(7;12)(q36;p13). Cancer Res 2001;61:5374–7.

[7] Simmons HM, Oseth L, Nguyen P, O'Leary M, Conklin KF, Hirsch B. Cytogenetic and molecular heterogeneity of 7q36/12p13 rearrangements in childhood AML. Leukemia 2002;16:2408–16.

[8] Tosi S, Hughes J, Scherer SW, Nakabayashi K, Harbott J, Haas OA, Cazzaniga G, Biondi A, Kempski H, Kearney L. Heterogeneity of the 7q36 breakpoints in the t(7;12) involving *ETV6* in infant leukemia. Genes Chromosomes Cancer 2003;38:191–200.

[9] Shimada A, Taki T, Tabuchi K, Tawa A, Horibe K, Tsuchida M, Hanada R, Tsukimoto I, Hayashi Y. *KIT* mutations, and not *FLT3* internal tandem duplication, are strongly associated with a poor prognosis in pediatric acute myeloid leukemia with t(8;21): a study of the Japanese Childhood AML Cooperative Study Group. Blood 2006;107:1806–9.

[10] Taketani T, Taki T, Sugita K, Furuichi Y, Ishii E, Hanada R, Tsuchida M, Sugita K, Ida K, Hayashi Y. *FLT3* mutations in the activation loop of tyrosine kinase domain are frequently found in infant ALL with *MLL* rearrangements and pediatric ALL with hyperdiploidy. Blood 2004;103:1085–8.

[11] Inoue K, Ogawa H, Yamagami T, Soma T, Tani Y, Tatekawa T, Oji Y, Tamaki H, Kyo T, Dohy H, Hiraoka A, Masaoka T, Kishimoto T, Sugiyama H. Long-term follow-up of minimal residual disease in leukemia patients by monitoring *WT1* (Wilms tumor gene) expression levels. Blood 1996;88:2267–78.

[12] Taketani T, Taki T, Shibuya N, Kikuchi A, Hanada R, Hayashi Y. Novel *NUP98–HOXC11* fusion gene resulted from a chromosomal break within exon 1 of *HOXC11* in acute myeloid leukemia with t(11;12)(p15;q13). Cancer Res 2002;62:4571–4.

[13] Deguchi Y, Kehrl JH. Selective expression of two homeobox genes in CD34-positive cells from human bone marrow. Blood 1991;78: 323–8.

[14] Deguchi Y, Yamanaka Y, Theodossiou C, Najfeld V, Kehrl JH. High expression of two diverged homeobox genes, HB24 and HB9, in acute leukemias: molecular markers of hematopoietic cell immaturity. Leukemia 1993;7:446–51.

[15] Harrison KA, Druey KM, Deguchi Y, Tuscano JM, Kehrl JH. A novel human homeobox gene distantly related to proboscipedia is expressed in lymphoid and pancreatic tissues. J Biol Chem 1994;269: 19968–75.

THE JOURNAL OF BIOLOGICAL CHEMISTRY VOL. 283, NO. 39, pp. 26820–26828, September 26, 2008


# Fusion of OTT to BSAC Results in Aberrant Up-regulation of Transcriptional Activity*[S]

Received for publication, March 25, 2008, and in revised form, July 21, 2008 Published, JBC Papers in Press, July 30, 2008 DOI 10.1074/jbc.M802315200

**Taisuke Sawada[‡], Chiharu Nishiyama[§], Takuma Kishi[‡], Tomonari Sasazuki[‡], Sachiko Komazawa-Sakon[‡], Xin Xue[‡], Jiang-Hu Piao[‡¶‖], Hideko Ogata[‡], Jun-ichi Nakayama[**], Tomohiko Taki[‡‡], Yasuhide Hayashi[§§], Mamoru Watanabe[¶¶], Hideo Yagita[‡], Ko Okumura[‡], and Hiroyasu Nakano[‡1]**

*From the [‡]Department of Immunology, [§]Atopy (Allergy) Research Center, and [¶]Sportology Center, Juntendo University School of Medicine, 2-1-1 Hongo, Bunkyo-ku, Tokyo 113-8421, Japan, the [‖]Department of Immunology, School of Basic Medical Science, Ningxia Medical College, Xingqing-Qu, Yinchuan 750004, China, the [**]Laboratory for Chromatin Dynamics, Center for Developmental Biology, RIKEN, 2-2-3 Minatojima-Minamimachi, Chuo-ku, Kobe 650-0047, Japan, the [‡‡]Department of Molecular Laboratory Medicine, Kyoto Prefectural University of Medicine Graduate School of Medical Science, 465 Kajii-cho kawaramachi-Hirokoji, Kamigyo-ku, Kyoto 602-8566, Japan, the [§§]Gunma Children's Medical Center, 779 Shimohakoda, Kitatachibana, Gunma 377-8577, Japan, and the [¶¶]Department of Gastroenterology and Hepatology, Tokyo Medical and Dental University, 1-5-45 Yushima, Bunkyo-ku, Tokyo 113-8519, Japan*

***OTT/RBM15-BSAC/MAL/MKL1/MRTF-A* was identified as a fusion transcript generated by t(1;22)(p13;q13) in acute megakaryoblastic leukemia. Previous studies have shown that BSAC (basic, SAP, and coiled-coil domain) activates the promoters containing CArG boxes via interaction with serum response factor, and OTT (one twenty-two) negatively regulates the development of megakaryocytes and myeloid cells. However, the mechanism by which OTT-BSAC promotes leukemia is largely unknown. Here we show that OTT-BSAC, but not BSAC or OTT strongly activates several promoters containing a transcription factor Yin Yang 1-binding sequence. In addition, although BSAC predominantly localizes in the cytoplasm and its nuclear translocation is considered to be regulated by the Rho-actin signaling pathway, OTT-BSAC exclusively localizes in the nucleus. Moreover, OTT interacts with histone deacetylase 3, but this interaction is abolished in OTT-BSAC. Collectively, these functional and spatial changes of OTT and BSAC caused by the fusion might perturb their functions, culminating in the development of acute megakaryoblastic leukemia.**

Transcriptional activation of many genes depends on activities of the transcriptional factors that recognize specific target sequences but also the chromatin structures. Histone acetyltransferases and histone deacetylases (HDACs)[2] are recruited to target genes through association with specific transcriptional factors (1, 2). Histone acetyltransferases relax chromatin structures and activate transcription by acetylating histones, whereas HDACs condense chromatin structures and repress transcription by deacetylating histones (1, 2). So far, there have been three HDAC families identified (3). Class I HDACs (HDAC1, -2, -3, and -8) are closely related to the yeast transcriptional regulator RPD3 and expressed in most cell types. Class II HDACs (HDAC4, -5, -6, -7, -9, and -10) share domains with a similarity to HDA1, another deacetylase in yeast. Class III HDACs are related to the yeast silencing protein SIR2 and are dependent on NAD for enzymatic activity. HDACs exist in cells as a part of large molecular weight complex containing adaptor molecules, including Sin3A, SMRT (silencing mediator for retinoid and thyroid receptors), N-CoR (nuclear receptor corepressor), and/or SHARP (SMRT and HDAC1-associated repressor protein) (4). SHARP belongs to a family of RNA recognition motif proteins and also has a SMRT-interacting domain at the C terminus, which mediates the interaction with SMRT, N-CoR, and HDACs (5). The SMRT-interacting domain is also characterized as a SPOC (spen paralog and ortholog C-terminal) domain that was found in *Drosophila* spen and spen-like protein (6).

The t(1;22)(p13;q13) is exclusively associated with infant acute megakaryoblastic leukemia. Two groups have been independently identified as a fusion transcript that is generated by this chromosomal translocation and composed of two novel genes, designated OTT (one twenty-two) or RNA-binding motif protein (RBM) 15 and megakaryocytic acute leukemia (MAL) or megakaryoblastic leukemia-1(MKL1) (7, 8). OTT contains three RNA recognition motifs and SPOC domain (7, 8), whereas MAL is composed of N-terminal basic, glutamine-

* This work was supported in part by a Grant-in-Aid for a "High-Tech Research Center" Project for Private Universities, matching fund subsidy from the Ministry of Education, Culture, Sports, Science and Technology, and Scientific Research (B) and (C) from Japan Society for the Promotion of Science, and grants from the NOVARTIS Foundation (Japan) for the Promotion of Science, the Takeda Science Foundation, the Mitsubishi Pharma Foundation, and the Tokyo Biochemical Research Foundation. The costs of publication of this article were defrayed in part by the payment of page charges. This article must therefore be hereby marked "*advertisement*" in accordance with 18 U.S.C. Section 1734 solely to indicate this fact.

[S] The on-line version of this article (available at http://www.jbc.org) contains supplemental Fig. S1.

[1] To whom correspondence should be addressed: Dept. of Immunology, Juntendo University School of Medicine, 2-1-1 Hongo, Bunkyo-ku, Tokyo 113-8421, Japan. Tel.: 81-3-5802-1045; Fax: 81-3-3813-0421; E-mail: hnakano@juntendo.ac.jp.

[2] The abbreviations used are: HDAC, histone deacetylase; ChIP, chromatin immunoprecipitation; YY1, Yin Yang 1; MAL, megakaryocytic acute leukemia; MKL1, megakaryoblastic leukemia-1; RBM, RNA-binding motif protein; GPVI, platelet collagen receptor glycoprotein VI; EMSA, electrophoretic mobility shift assay; SRF, serum response factor; siRNA, small interfering RNA; TA, transcriptional activation.